

OUTER BILLIARDS WITH CONTRACTION

IN-JEE JEONG

ABSTRACT. We study the dynamics of outer billiards with contraction outside polygons. The dynamics can be either regular or chaotic, depending on the parameters.

CONTENTS

1. Introduction	1
2. Definitions and Preliminary Results	2
3. Dynamics Outside the Square	5
4. Types of Periodic Orbits	9
4.1. Fagnano-type Periodic Orbits	10
4.2. Stable Periodic Orbits	11
4.3. Stable Degenerate Periodic Orbits in Trapezoids	14
4.4. Star Shaped Periodic Orbits in Regular Polygons	18
4.5. Periodic Orbits of Winding Number 1 in Quadrilaterals	20
5. Analysis of the Triangular Transition	22
5.1. Preview	22
5.2. Attracting Cantor Sets	23
5.3. Degenerate Periodic Orbits	25
Acknowledgments	28
Appendix A. Proof of Theorem 25.	29
Appendix B. Rotation Theory for Discontinuous Circle Maps	32
References	33

1. INTRODUCTION

The outer billiards map, popularized by Moser in his article [7], is a major example of a dynamical system. It has been studied by various people and while [17], [19] are good references (the latter written primarily for undergraduates), a few important results were obtained afterwards; for example, see [14, 13]. Look at the pictures of the periodic tiles of the outer billiards map outside some regular polygons! These beautiful pictures (produced by R. Schwartz) are enough motivation to study this system.

In this thesis, we modify the construction to get a contractive map which we call as “outer billiards with contraction,” see Figure 2.1. The dynamical system is determined by a pair (P, λ) where P is a convex polygon and λ is the contraction factor between 0 and 1. Let us list the main questions that we are interested in.

- Regarding periodic orbits: Is there exist a periodic orbit? Is the number of periodic orbits always finite?
- Regarding asymptotic behavior of points: Is every orbit asymptotic to a periodic orbit? If not, what are possible asymptotic behaviors?

Experiments strongly suggest that for a randomly chosen pair (P, λ) , there exist only finitely many periodic orbits to which all other orbits are attracted. Indeed, it is expected from a “generic” piecewise contracting map that the dynamics is “regular.” Two articles [2, 9] have established results of this kind. They also give several motivation to study piecewise contractions. In [2], authors study a large class of piecewise contractions on the plane and show that for almost every choice of parameters, any orbit is attracted to a periodic orbit. On the

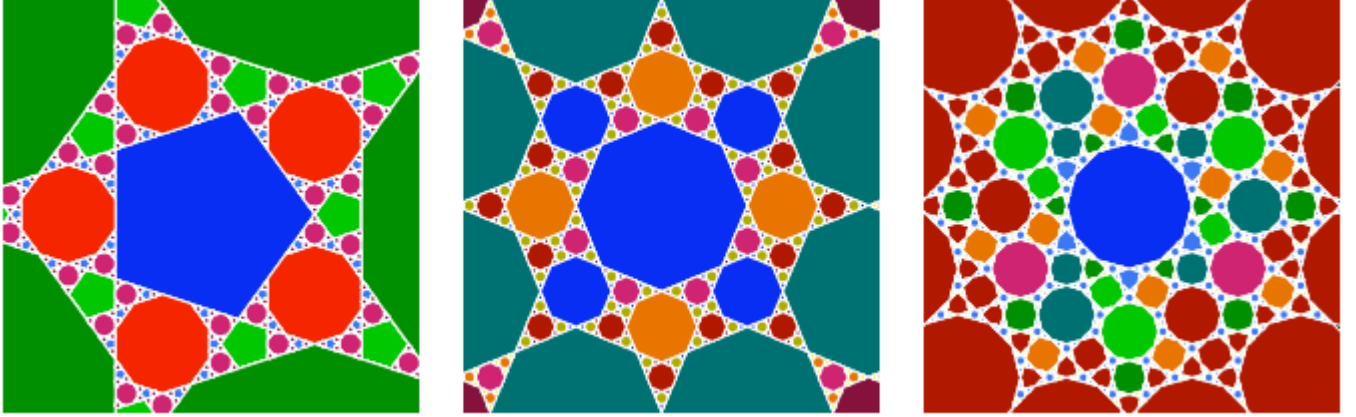


FIGURE 1.1. Dynamics of the outer billiards map outside regular 5, 8, and 12-gons (taken from the website <http://icerm.brown.edu/>)

other hand, in [9], authors consider piecewise contractions on the interval and show that there are at most n periodic orbits where n is the size of the partition. Moreover, when the map has n periodic orbits, every orbit is attracted to a periodic one.

The goal of this thesis is to introduce a wide variety of phenomena occurring in this dynamical system. We hope to convince you that the dynamics depends in subtle ways to the geometry of P . One can view this thesis as a gallery where picture has an accompanying mathematical description. It is more fun to look at those pictures if you know mathematical stories behind them.

The remainder of this thesis is divided into four sections. In Section 2, we discuss very basic properties of the system. In Section 3, we will analyze the dynamics when the polygon is a square; the dynamics has a simple description, but still quite interesting. Then Section 4 discusses various types of periodic orbits that we can observe for specific families of polygons. Finally in Section 5, we show that for some polygons, an attracting Cantor set exists; that is, the dynamics can be chaotic.

2. DEFINITIONS AND PRELIMINARY RESULTS

To define our dynamical system rigorously, we fix a convex polygon P in the plane and a number $0 < \lambda < 1$. Given a point x outside of P , we draw the ray from x to a vertex y of P such that P lies on the left side of this ray. Now we can find the unique point z on the other side of the ray with respect to x such that $|xy| : |yz| = 1 : \lambda$. We denote this transformation $x \mapsto z$ by T_λ , suppressing the dependence of the map on P . Letter T will be reserved for the standard outer billiards map.

Note that this map is well-defined except for a finite union of rays S which extends sides of P . Then we note that away from a measure zero set (which is a countable union of rays), T_λ can be iterated infinitely many times. Then we simply take out this measure zero set from our domain so that T_λ defines a dynamical system. That is, the domain can be written as $X := \mathbb{R}^2 \setminus (P \cup (\cup_{i=0}^{\infty} T_\lambda^{-i} S))$.

In this section, we are going to prove:

- (1) All regular periodic orbits are attracting, and no degenerate periodic orbit of odd period is attracting
- (2) The explicit formula for the coordinates of the periodic orbit given a combinatorics
- (3) All the asymptotic dynamics is happening in a bounded ball

We say that a point $x \in X$ is periodic of period n if $T_\lambda^n(x) = x$ and $T_\lambda^m(x) \neq x$ for $1 < m < n$. Corresponding periodic orbits is $\mathcal{O}(x) = \{x, \dots, T_\lambda^{n-1}x\}$. Often we call such an orbit regular periodic orbit to emphasize that $\mathcal{O}(x) \subset X$. We will see shortly that any regular periodic orbit is locally attracting; that is, there exists an open set $O \subset X$ such that for all $a \in O$, there exists m such that $|T_\lambda^{m+nk}a - x| \rightarrow 0$ as $k \rightarrow \infty$, if the periodic orbit were generated by x . Next, we note that for points on the singular ray S , there are two natural choices for T_λ

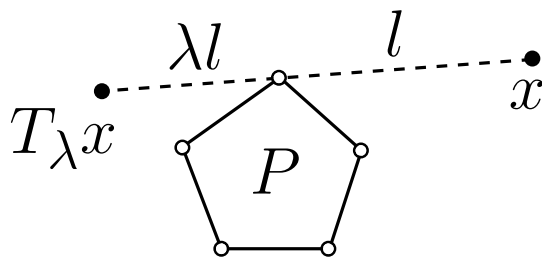


FIGURE 2.1. Outer billiards with contraction

that can make T_λ continuous at least from one side. Moreover, there is one natural choice for T_λ for points on the sides of P .

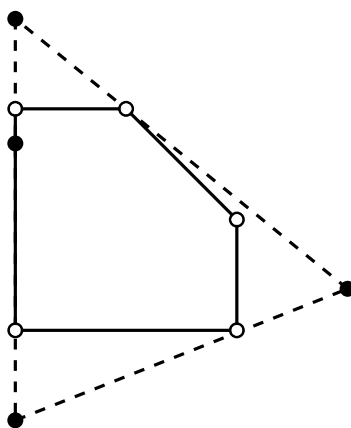


FIGURE 2.2. An attracting degenerate periodic orbit

Then we say that a finite sequence of points $\{x_1, \dots, x_n\} \subset \text{cl}(\mathbb{R}^2 \setminus P)$ is a degenerate periodic orbit if for each $1 \leq i \leq n$, $T_\lambda x_i = x_{i+1}$ whenever $T_\lambda x_i$ is well-defined and otherwise (that is, when x_i is on S or on the sides of P), x_{i+1} should be one of natural choices of T_λ for x_i . With this definition, there are plenty of degenerate periodic orbits for any pair (P, λ) ; for an extreme example, each vertex of P is always a degenerate fixed point. However, a degenerate periodic orbit is interesting only when some points in our domain X is asymptotic to it. This phenomenon never happens in ordinary outer billiards (due to its piecewise isometric nature). Here we give a concrete example of an attracting degenerate periodic orbit; see Figure 2.2. Take P to be the “truncated square” with vertices $(0, 0)$, $(1, 0)$, $(1, 0.5)$, $(0.5, 1)$, and $(0, 1)$, and $\lambda = 0.5$. Then the sequence $\{(0, 1.4), (0, 0.8), (0, -0.4), (1.5, 0.2)\}$ is a period-4 degenerate periodic orbit. Notice that a point lies on a side of P . We claim that the whole domain X is asymptotic to this periodic orbit, fully justifying the necessity of considering degenerate periodic orbits. We do not prove this claim as it can be done by a finite amount of calculation.

It is a basic fact that the dynamics of outer billiards (with or without contraction) is invariant under affine transformations. To be more precise, if there exists an affine transformation of the plane (which has the form $x \mapsto Ax + x_0$ where A is a 2×2 matrix and x_0 is a fixed vector) which sends a polygon P to another polygon Q , then the dynamics for (P, λ) is conjugate to the dynamics for (Q, λ) . We note that up to affine transformations, there exists a unique triangle, a unique parallelogram, one parameter family of trapezoids, and two parameter family of quadrilaterals.

We recall a very well-known lemma from analysis. We say that a point p is asymptotic to a fixed point y if $|T^n p - y| \rightarrow 0$ as $n \rightarrow \infty$.

Lemma (Contraction Lemma). *Let Y be a complete metric space and $f : Y \rightarrow Y$ be a contraction. Then there exists a unique fixed point that every point in Y is asymptotic to.*

The following is just an analogous statement to the fact that in any piecewise isometric system (in Euclidean spaces), when we have a periodic orbit, there exists a periodic polygonal open set around the orbit (which is often called a tile).

Lemma 1. *Any regular periodic orbit is attracting, while a degenerate periodic orbit of odd period is never attracting.*

Proof. To prove the first statement, fix a point x inside the periodic orbit and assume its period is n . Let the sequence of vertices of P that x hits via iteration of T_λ be $\{v_1, \dots, v_n\}$. Let Y be the subset of $\mathbb{R}^2 \setminus P$ such that T_λ is well-defined at least until n iterations and hits the same sequence of vertices with x . It is easy to see that Y is an open convex polygon (as it is an intersection of finite half-planes) and that x is contained in Y . Since x is a fixed point of T_λ^n , and T_λ^{2n} is also orientation-preserving, we know that $T_\lambda^{2n}(Y) \subset Y$, defining a contraction on a complete metric space Y . Therefore, we are done by the contraction lemma.

For the second statement, let \mathcal{O} be a degenerate periodic orbit of odd period n , and it is easy to see that there always exists a point $x \in \mathcal{O} \cap S$. Assume on the contrary that there exists a open set U that is asymptotic to this periodic orbit. We can assume that the closure of U contains x . We first observe that the singular ray S cuts any small open ball containing x into two half-open balls and that U should be necessarily contained in one of two sides. But on U , at least for a.e. points, iterations of T_λ are well-defined. However, a composition of odd number of orientation-reversing maps is orientation-reversing, so $T_\lambda^n U$ is always contained on the other side of U with respect to S . Since the rule for T_λ is completely different on the other side, $T_\lambda^{n+1} U \not\subset T_\lambda U$, which is a contradiction. \square

We note that some degenerate periodic orbits of even period are attracting, while some are not. It depends on how the orbit wraps around P . We already gave an example of an attracting degenerate periodic orbit, and we will see non attracting degenerate periodic orbits of even period in Section 3.

Given a point $x \in X$, we can look at the sequence of vertices $\{v_1, v_2, \dots\}$ it hits when we iterate T_λ . Such a sequence will be often called the combinatorics of x . Any sequence of vertices will be also called a combinatorics. This sequence being periodic forces x to be a periodic point via the contraction lemma. On the other hand, given a finite combinatorics $\{v_1, \dots, v_n\}$, we are curious if there is a periodic point x (regular or not) realizing this combinatorics. The next lemma gives an answer, and since for any N there are only finitely many combinatorics of length N , it is theoretically possible to locate all periodic orbits of period less than N .

Lemma 2. *For any P and any finite combinatorics $\{v_i\}_{i=0}^{n-1}$, there exists at most one periodic point realizing it, whose coordinates (if exists) are determined by the formula*

$$(2.1) \quad q(\lambda) = \frac{1 - (-\lambda)}{1 - (-\lambda)^n} \left(\sum_{i=0}^{n-1} (-\lambda)^{n-1-i} v_i \right).$$

Proof. Consider the map $\Phi = T_{n-1} \circ T_{n-2} \circ \dots \circ T_0$, where T_i is the reflection with respect to the vertex v_i composed with contraction by λ . Then clearly, Φ is a contraction of the form $p \mapsto (-\lambda)^n p + (1 + \lambda) \left(\sum_{i=0}^{n-1} (-\lambda)^{n-1-i} v_i \right)$. If we assume that a periodic point exists, it must be a fixed point of this contraction which is unique. By letting $p = \Phi p$, we get the desired formula. \square

Therefore, a combinatorics is realized if and only if each point in the sequence $\{q(\lambda), T_\lambda q(\lambda), \dots, T_\lambda^{n-1} q(\lambda)\}$ is located ‘‘correctly’’ on $\mathbb{R}^2 \setminus P$ with respect to the partition by S . The formula for $q(\lambda)$ itself will be used repeatedly in the following sections.

Now we show that all the interesting dynamics happens in a bounded ball. This shows a striking contrast with standard outer billiards, in which boundedness question is wide open for a generic P . Intuitively, if $x \in X$ is very far (in terms of the size of P and λ) away from P , it is conceivable that $d(T_\lambda x, P) < \mu d(x, P)$ for some uniform factor $\lambda < \mu < 1$.

Lemma 3. *Given (P, λ) , there exists a ball B of radius not exceeding $\frac{1+\lambda}{1-\lambda} \max_i |v_i|$ such that $T_\lambda(B \cap X) \subset B$ and for any $x \in X$, there exists $N > 0$ such that $T_\lambda^N x \in B$.*

Proof. A simple computation. □

Finally, we can conclude that a (regular) periodic orbit is not destroyed under small perturbation of the polygon or λ . If P is an n -gon, we assume that the vertices are cyclically ordered and regard it as a point in \mathbb{R}^{2n} . Then we can talk about the distance between two (ordered) n -gons. In the following lemma, P and P' will need to have the same number of vertices.

Lemma 4 (Stability of periodic orbits). *Let \mathcal{O} be a periodic orbit for (P, λ) . Then there exists $\epsilon > 0$ depending on \mathcal{O}, P, λ such that if the pair (P', λ') is ϵ -close to (P, λ) , then there exists a periodic orbit \mathcal{O}' for (P', λ') which has the same combinatorics with \mathcal{O} .*

Proof. We only need to observe that the Equation 2.1 and the continuity regions for T_λ vary continuously in vertices of the polygon and the contraction factor. □

3. DYNAMICS OUTSIDE THE SQUARE

In this section, we analyze the dynamics when P is a square (or equivalently, a parallelogram) and conclude that the dynamics is nicest possible. For now, just note from Figure 3.3 that for different value of λ , there exists different number of periodic orbits (each color corresponds to the basin of attraction for a periodic orbit).

Let us outline the proof of the Theorem 6. Recall that without contraction, the outer billiards map outside a square just permutes the open squares of the same label in Figure 3.1, and every point inside a square of index k is periodic with period $4k$. Then now with contraction, define the index of a point to be the index of the square that the point belongs to. When the point is adjacent to two or more squares, we can set the index to be the minimum. Then we note that under the dynamics T_λ , the index of a point never increases. In particular, it must stabilize to some k , and after it stabilizes, it should follow the combinatorics of the standard outer billiards map. Therefore, with the Equation 2.1, we can explicitly compute the coordinates of the asymptotic limit, and we argue that the k th T_λ -periodic orbit exists if and only if this limit point lies in the “right” region (namely in the interior of a square of index k). We will conclude that it exists precisely when $\lambda \in (\lambda_k, 1)$ for some number λ_k .

4	3	2	3	4
3	2	1	2	3
2	1		1	2
3	2	1	2	3
4	3	2	3	4

FIGURE 3.1.

For concreteness, we arrange that the four vertices of our square have coordinates $(\pm 1, \pm 1)$. We first prove a simple algebraic lemma.

Lemma 5. *For $k \geq 1$, the polynomial $p_k(\lambda) = 1 - \lambda^{k-1} - \lambda^k + \lambda^{2k}$ has a unique root in $[0, 1)$ which we denote by λ_k . Then the sequence $\{\lambda_k\}_{k \geq 1}$ is strictly increasing with limit 1.*

Proof. When $k = 1$, $p_k(\lambda) = -\lambda + \lambda^2$ and $\lambda_1 = 0$. Now assume $k \geq 2$. Since $p_k(0) = 1$ and $p_k(1) = 0$, it is enough to prove that there exists a point a_k such that p_k is decreasing in the interval $(0, a_k)$ and increasing in the interval $(a_k, 1)$. The derivative $p'_k(\lambda)$ has the form $-\lambda^{k-2}q_k(\lambda)$, so let us show $q_k(\lambda)$ has a unique root b_k in the interval $(0, 1)$ such that $q_k(\lambda) > 0$ when $0 < \lambda < b_k$ and $q_k(\lambda) < 0$ when $b_k < \lambda < 1$. The derivative $q'_k(\lambda) = k - 2k(k+1)\lambda^k$ is monotonic and has a unique root in $(0, 1)$. Since $q_k(0) = k - 1 > 0$ and $q_k(1) = -1 < 0$, we are done.

To prove $\lambda_k < \lambda_{k+1}$, since $p_k(\lambda) < 0$ only when $\lambda > \lambda_k$ in the interval $(0, 1)$, it is enough to check $p_k(\lambda_{k+1}) < 0$, which is elementary. Because $\lambda_k < 1$ for all k and λ_k is increasing, the limit of λ_k exists, which we denote by $l \leq 1$. From the equation

$$1 = \lim_{k \rightarrow \infty} l^{k-1}(1 + l - \lim_{k \rightarrow \infty} l^{k+1}),$$

one sees that $l = 1$. □

Theorem 6. *For all $\lambda_k < \lambda \leq \lambda_{k+1}$, there exists exactly k T_λ -periodic orbits to which all other orbits are attracted.*

Proof. Notice that with any $0 < \lambda < 1$, T_λ never increases the index of the square that the orbit of a point p lies on. Since the index cannot decrease indefinitely, we can assume that it stabilizes at some k . Notice that once it stabilizes, for each point in a k -square, there is a unique k -square that it can be mapped to. Moreover, it is possible to get from any k -square to any other one. Hence, pick an integer N such that $T_\lambda^N p$ lies on S_k , the (open) k -square with center $(-2k, 0)$. Now, the combinatorics of $T_\lambda^N p$ is fixed, which means that the iteration T_λ^{4k} is a fixed contraction, and therefore p must converge to the unique fixed point $q_k(\lambda)$ of T_λ^{4k} whose formula is given by Equation 2.1.

If, for some λ , it turns out that the formula for q_k does not give a point in $\text{cl}(S_k)$ (q_k can be on the boundary of S_k and still define an attracting periodic orbit), it means that for this value of λ , $4k$ T_λ -periodic orbit cannot exist. In the next two lemmas, we show the following statements. First, there exists a number λ_k which happens to be the root of $p_k(\lambda)$ in $[0, 1)$, such that $q_k \in \text{cl}(S_k)$ if and only if $\lambda \in [\lambda_k, 1)$. When $q_k \in S_k$, it defines a regular periodic orbit, and when $q_k \in \partial S_k$, it defines a degenerate periodic orbit which is non attracting. Hence, the proof is complete. □

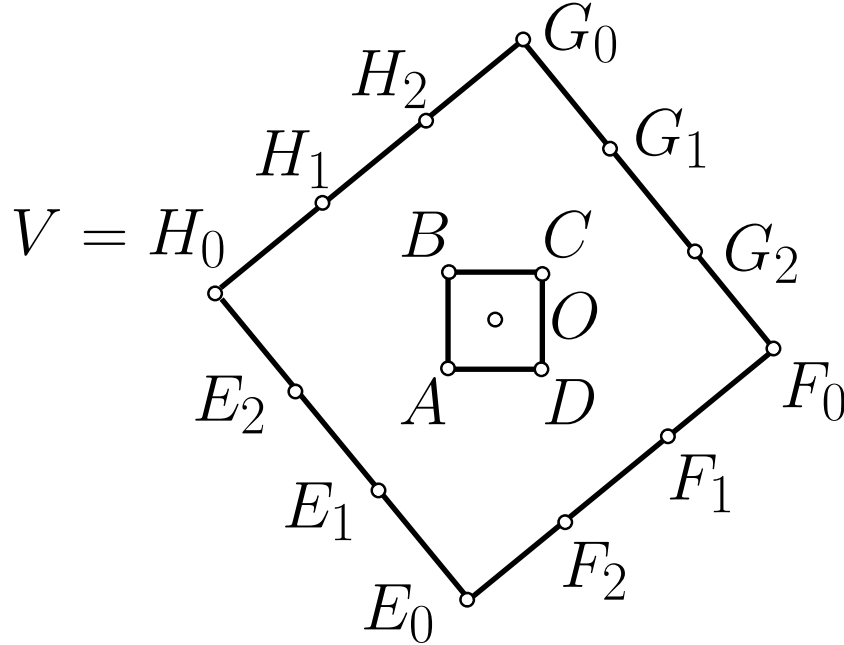


FIGURE 3.2. The third $T_{0.95}$ -periodic orbit

Lemma 7. For all $0 < \lambda \leq 1$, coordinates of the point $q_k(\lambda) = (x(\lambda), y(\lambda))$ has the following explicit formula:

$$x(\lambda) = \frac{-(1+\lambda)(1-\lambda^{2k})}{(1-\lambda)(1+\lambda^{2k})} \quad y(\lambda) = \frac{(1+\lambda)(1-\lambda^k)^2}{(1-\lambda)(1+\lambda^{2k})}.$$

Proof. Since each vertex v_i of the square has coordinates ± 1 , we can encode the combinatorics of each coordinate by a sequence of $+$ and $-$. Then we have $x(\lambda) = (\sum \lambda^{4k-1-i} (-1)^{i-1} v_{x,i}) (1+\lambda) / (1-\lambda^{4k})$ where $v_{x,i}$ is either $+1$ or -1 . The sign of $v_{x,i}$ alternates, except for precisely two cases when the orbit goes through a horizontal square. Since our point p is in a horizontal square, $\{v_{x,i}\}$ has the form $- + - \dots + \dots - + -$, where by symmetry two consecutive $+$ occurs at the $2k$ and $2k+1$ positions. By multiplying this sequence with $(-1)^{i-1}$, we have a simple pattern where $2k$ pluses are followed by $2k$ minuses. Therefore, we have the sum $\sum \lambda^{4k-1-i} (-1)^{i-1} v_{x,i} = \sum_{j=0}^{2k-1} \lambda^{2k} \lambda^j - \sum_{j=0}^{2k-1} \lambda^j$ which gives us the formula for $x(\lambda)$. Similarly, $v_{y,i}$ has the alternating combinatorics except for two spots where the orbit goes through a vertical square. Multiplying it with $(-1)^{i-1}$, we get the sequence where we have k pluses at both ends surrounding $2k$ minuses. For an example, we have $++-----++$ when $k=2$. Explicitly adding the geometric series gives us the formula for $y(\lambda)$. These formulas are easily seen to be convergent when $\lambda \rightarrow 1$. \square

Lemma 8. The limit curve $q_k(\lambda)$ defines a $4k$ -periodic point under T_λ if and only if $\lambda > \lambda_k$.

Proof. This lemma will show that for $\lambda_k < \lambda \leq \lambda_{k+1}$, there are exactly k periodic orbits.

Given the point $q_k(\lambda) := H_0$ for a fixed λ , we construct other $4k-1$ points. We rotate H_0 with respect to the origin O by $\pi/2, \pi, 3\pi/2$ to obtain points E_0, F_0 , and G_0 . (Figure 3.2) On the segment H_0E_0 , we pick points $E_{k-1}, E_{k-2}, \dots, E_1$ so that the lengths of sides $E_{j+1}E_j$ satisfy $|E_{j+1}E_j|/|E_jE_{j-1}| = \lambda$ for all $1 \leq j \leq k-1$ ($E_k = H_0$). Then we construct points F_j, G_j, H_j similarly that $4k$ points have $\pi/2$ -rotational symmetry with respect to the origin.

Let us proceed to show that if $\lambda \geq \lambda_k$, these $4k$ points form a periodic orbit. First we show that the points E_{k-1}, \dots, E_0 gets reflected on the vertex D . (which is enough by rotational symmetry) Since they are collinear, it is enough to show that the y coordinate of E_{k-1} is less than or equal to -1 and the x coordinate of E_0 is less than or equal to 1 . We use the formulas from Lemma 7. It is apparent that the y -coordinate of H_0 is positive, so the x coordinate of E_0 is indeed less than 0 (stronger than what we need) by symmetry. Next, it is a simple computation to show that the y coordinate of E_{k-1} equals the convex combination

$$\hat{y}(\lambda) = \frac{1-\lambda^{k-1}}{1-\lambda^k} y(\lambda) + \frac{\lambda^{k-1}-\lambda^k}{1-\lambda^k} x(\lambda)$$

and we solve for the condition $\hat{y} \leq -1$. It turns out that it holds if and only if $1 - \lambda^{k-1} - \lambda^k + \lambda^{2k} \leq 0$ which happens precisely in the interval $[\lambda_k, 1)$. Therefore, if $\lambda < \lambda_k$, there cannot exist a periodic orbit in k th squares.

It remains to show that these $4k$ points are T_λ -invariant. Indeed, we claim that it is enough to check that $T_\lambda H_0 = F_1$. Consider two triangles $\triangle H_0 H_1 A$ and $\triangle F_1 F_2 A$. Since H_0, A, F_1 are shown to be collinear and segments $H_0 G_0$ and $E_0 F_0$ are parallel, $\angle H_1 H_0 A = \angle F_2 F_1 A$. Moreover, we have ratios $|H_0 A|/|F_1 A| = |H_0 H_1|/|F_1 F_2| = \lambda$ from our construction. Therefore, these triangles are similar, and $T_\lambda H_1 = F_2$. Likewise, $T_\lambda H_j = F_{j+1}$ for $j = 1 \dots k-1$, where $F_k = E_0$. By rotational symmetry, T_λ is indeed an orbit. Next, a direct computation establishes that $T_\lambda H_0 = F_1$.

Finally, we need to show that the degenerate periodic orbit formed by q_k when $\lambda = \lambda_k$ is non attracting. It is enough to show that no points inside two lattice squares adjacent to the singular point E_{k-1} converge to E_{k-1} . No points from the square above E_{k-1} certainly cannot converge to E_{k-1} since it reflects on A in the beginning. Next, we may assume that a small open set inside the lattice square below E_{k-1} , after $2k$ iterates of T_{λ_k} , becomes an open set touching the singular point G_{k-1} because otherwise we are done. However, since $2k$ is even, the latter open set lies below G_{k-1} and reflects on C rather than on B . \square

Remark 9. Notice from Equation 7 that the limit curve converges to the center of the square, $(-2k, 0)$ as $\lambda \rightarrow 1$. This phenomenon also happens for periodic domains of regular 3, 5, 6, 8-gons and will be obtained as a corollary of Theorem 13 later.

We have $\lambda_2 = 0.755\dots$, $\lambda_3 = 0.890\dots$. In Figure 3.3, the dynamics is drawn for three values of λ , 0.7, 0.8, and 0.9. In each picture, one notices that the domain is divided into many rectangles; each rectangle is the set of

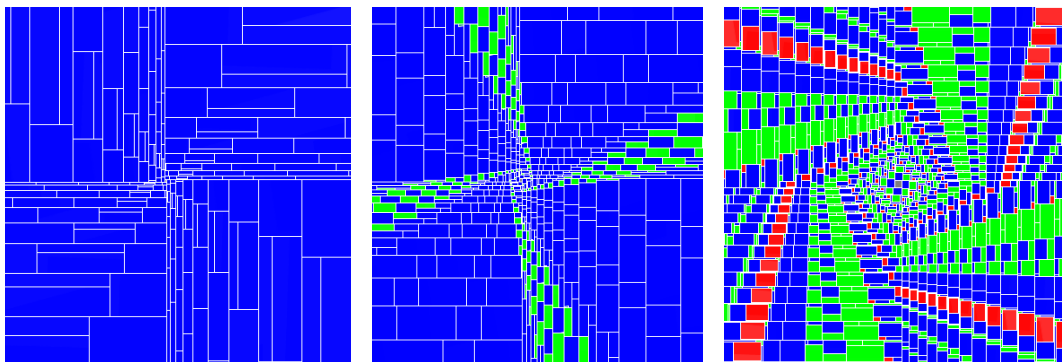


FIGURE 3.3. “Bird’s eye view” of dynamics outside the square for $\lambda = 0.7, 0.8, 0.9$ (from left to right)

points with the same combinatorics, and their boundaries are precisely the bad set we have taken out from our domain. First, $0.7 < \lambda_2$ so in the leftmost picture, we have one periodic orbit which attracts everything. Next, $\lambda_2 < 0.8 < \lambda_3$, so we see two periodic orbits in the second picture. The green region corresponds to the set of points that converge to the second periodic orbit. In the rightmost picture, we see the partition of the plane into three sets, corresponding to three periodic orbits. Notice that the proportion of the green region has increased compared to the second picture.

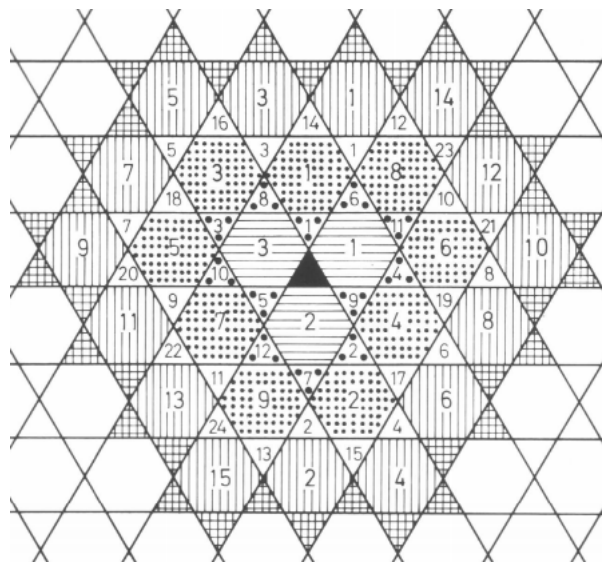


FIGURE 3.4. Outer billiards outside the equilateral triangle

We claim that similar analysis can be done for the triangle (unique up to affine transformation) and for the regular hexagon. For each of them, there exists a “graded” tiling of the plane enjoying the same properties. However, the analysis is more involved as there are two types of periodic orbits, hexagonal and triangular. See Figure 3.4 which is taken from Moser’s popular article [7]. Second, notice that when analyzing the periodic orbits for the square, we made a strong use of the fact that a whole periodic orbit lies on a square.

However, the conclusion is the same: each periodic domain for the outer billiards yields a T_λ -periodic domain if and only if λ exceeds a certain threshold. Therefore, it only remains to compute these thresholds to get the exact number of periodic orbits for given λ . We state the result when P is the triangle and omit its proof. One surprise is that the thresholds for hexagonal periodic orbits coincide with the odd threshold values λ_{2k-1} from the square case.

Claim 10. Indexed from inside, the k th hexagonal periodic domain has threshold λ_{2k-1} and the k th triangular periodic domain has threshold μ_k : for each $k \geq 1$, the polynomial $(x^{6k} - 1)(1 - x^{2k}) + (x^{4k-1})(1 - x)$ has a unique real root μ_k in the interval $(0, 1)$ which is strictly increasing and converges to 1 as $k \rightarrow \infty$. From this, we deduce that for any λ , there exists only finitely many periodic orbits (each coming from a periodic orbit from the standard outer billiards) to which all other orbits are attracted.

Let us summarize the common properties that dynamics outside three regular polygons have:

- (1) For any λ , there exists only finitely many periodic orbits to which every other orbits are attracted
- (2) For all λ , any periodic orbit comes from a T -periodic orbit
- (3) For each T -periodic orbit of P , there exists a threshold value $\lambda^* < 1$ such that this orbit gives a regular periodic orbit for (P, λ) precisely when $\lambda^* < \lambda < 1$.

We end this section by briefly mentioning the case when P is a regular pentagon. Without contraction, dynamics of the outer billiards map yields a beautiful fractal picture and is well-studied ([16, 8]). An extensive experiment with a computer program suggests the following conjecture:

Conjecture 11. *For the regular pentagon, all of the properties 1, 2, and 3 hold.*

It seems like that the 5-fold rotational symmetry of the regular pentagon forces T_λ -periodic orbits to be symmetric as well. In Figure 3.5, we have drawn the periodic domains outside the regular pentagon for some values of λ . If you look carefully, in first two pictures you see three periodic domains, while in the third one you see a tiny periodic domain (colored in red) appearing.

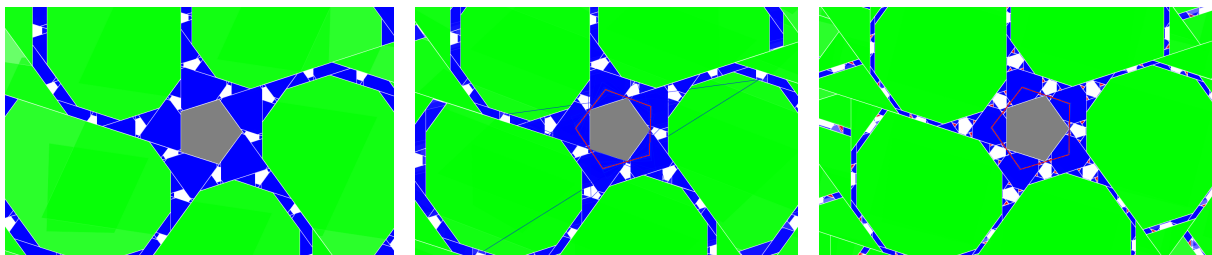


FIGURE 3.5. Dynamics outside the regular pentagon, when $\lambda = 0.89, 0.91$, and 0.95 (from left to right)

4. TYPES OF PERIODIC ORBITS

The aim of this section is to describe various types of periodic orbits for T_λ and study their properties; material in this section was primarily motivated to prove existence of periodic orbits for all (P, λ) . As a brief overview, we will describe and study four types of periodic orbits: (which will be defined in corresponding subsections)

- (1) Fagnano-type
- (2) Stable (under variations on λ)
- (3) Stable degenerate
- (4) Star shaped
- (5) Winding number 1

We briefly comment on the significance of each types of orbits. The first one exists for any polygon for sufficiently small λ (depending on the polygon) and provides a counterexample that all periodic orbits for (P, λ) come from periodic orbits without contraction. The stable periodic orbits enable us to conclude for some polygons that as $\lambda \rightarrow 1^-$, the number of periodic orbits diverges, as we have seen for three regular polygons. Moreover, the existence of non-stable periodic orbit points at the complexity of the outer billiards map outside the regular septagon. The third category of periodic orbits is not only interesting by its mere existence but we have observed (without proof) that for certain polygons (namely, lattice trapezoids), any periodic orbit (as λ varies from 0 to 1) is either type 1, 2, or 3. The fourth one is a family of special periodic orbits for regular polygons. Finally, studying periodic orbits of winding number 1 is an attempt to prove that for any pair (P, λ) , there exists a periodic orbit. Interestingly, this analysis was a stepping stone of the proof of the nonexistence of periodic orbits for certain pairs (P, λ) which we discuss in Section 5.

4.1. Fagnano-type Periodic Orbits. In [18], Tabachnikov studies periodic orbits of outer billiards that hits each vertex of P exactly once in cyclic order. Following his terminology, we will call such a periodic orbit as Fagnano orbit. We also require this periodic orbit to be regular. We begin with an observation that if such an orbit exists, it should be unique, simply because the coordinates of its points should be given by Equation 2.1. Moreover, if P is a regular polygon, then the (familiar) Fagnano orbit exists for all $0 < \lambda < 1$.

F. Bozgan first observed and proved that for any P , for small enough λ there exists a Fagnano orbit. We will state his theorem and provide a short proof.

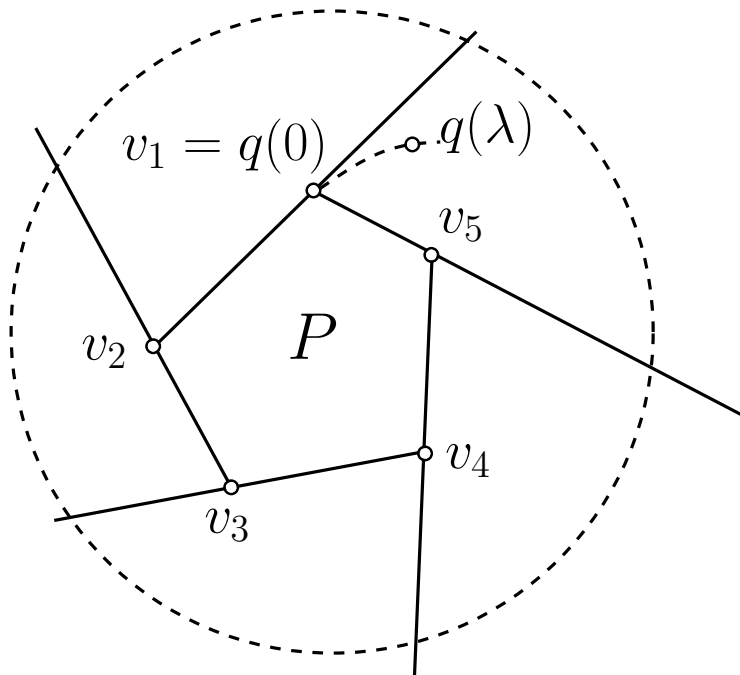


FIGURE 4.1. Proof of the Fagnano orbit theorem

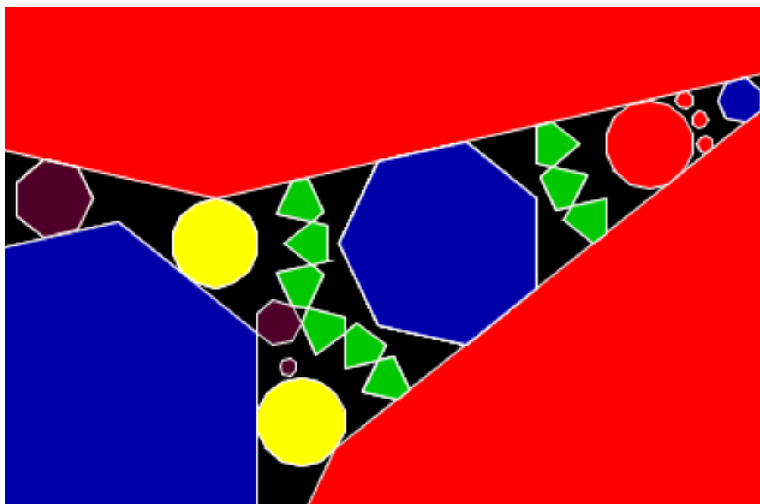
Theorem 12 (F. Bozgan). *For any P , there exist two threshold values $0 < \lambda'$ and $0 < \lambda'' \leq \lambda'$ such that for $\lambda \in (0, \lambda')$, the (regular) Fagnano orbit exists and for $\lambda \in (0, \lambda'')$, every orbit is attracted to the Fagnano orbit.*

Proof. We first prove the existence statement. Given P , we label the vertices counterclockwise from a vertex v_1, \dots, v_n , and we are looking for a periodic orbit with periodic combinatorics $\{v_1, \dots, v_n\}$. It exists if and only if $q(\lambda), T_\lambda q(\lambda), \dots, T_\lambda^{n-1} q(\lambda)$ lies on the interior of respective continuity regions. Therefore, it will be enough to prove that for λ sufficiently close to 0, the rational curve $q(\lambda)$ lies on the continuity region for v_1 as illustrated in Figure 4.1. From elementary geometry, it is enough to establish the following: (assuming $v_1 = 0$ for simplicity)

- $q'(0) = v_1 - v_2 = -v_2$
- $\frac{d}{d\lambda}|_{\lambda=0}\{(v_1 - v_2) \times (q(\lambda) - v_1)\} = -\frac{d}{d\lambda}|_{\lambda=0}(v_2 \times q(\lambda)) = -v_2 \times v_2 < 0$

And one can check both facts explicitly. Next, we prove the second statement. Notice from the formula for the invariant ball (Lemma 3) that if a ball B is invariant for (P, λ) then it is also invariant for all $\lambda' < \lambda$. Therefore, we take a ball that works for $\lambda = 1/2$, for example. This ball cuts the domain into n pieces as shown in Figure 4.1. It is trivial that for λ' small enough, the $T_{\lambda'}$ -image of each piece gets contained in the next piece. Since any orbit eventually gets into this ball, and once it gets into its combinatorics is fixed, we conclude that any orbit is asymptotic to the Fagnano orbit. \square

Note that the second step alone is not sufficient to prove that the Fagnano orbit is regular; some estimates on $q(\lambda)$ are essential. The trapezoid with the ratio of two bases equal to 2 does not have a Fagnano orbit without contraction. Therefore, it is not true that all periodic orbits for (P, λ) comes from a T -periodic orbit.

FIGURE 4.2. A non-stable T -periodic orbit for the regular heptagon

4.2. Stable Periodic Orbits. Let us let \mathcal{O} be a T -periodic orbit outside a polygon P . We say that \mathcal{O} is stable (to be precise, we should say λ -stable) if for λ sufficiently close to 1, the combinatorics of \mathcal{O} gives a T_λ -periodic orbit outside P . It might seem like that every T -periodic orbit is stable, so we start with a possible counterexample. Figure 4.2 shows some portion of the tiling of the plane by T -periodic tiles outside the regular septagon (which is not shown). We see a series of green pentagons of period 57848 which are indeed extremely small compared to the regular septagon P . These pentagons, along with many exotic periodic tiles outside the regular septagon were revealed by the computer program developed by R. Schwartz. Computer calculations suggest that these green pentagons is not stable under variations on λ .

Let us introduce the criterion we have used in this situation. Pick any of 57848 pentagons, and look at its combinatorics, which is just some sequence of vertices of the regular septagon of length 57848. If there were a T_λ -periodic orbit with this combinatorics, the corresponding point $q(\lambda)$ should be given by Equation 2.1. And if this green pentagon were stable, $\lim_{\lambda \rightarrow 1^-} q(\lambda)$ should be contained in the green pentagon we have picked. The computation shows that this limit was quite far away from the pentagon, so we are quite confident that this is non-stable (an exact arithmetic will verify this rigorously).

Although this is a necessary and sufficient condition, it does not explain the seemingly natural fact that when P is a square, $\lim_{\lambda \rightarrow 1^-} q(\lambda)$ was the center of each square. Computer experiments showed the same phenomenon obviously for the triangle but also for the regular pentagon.

This can be explained by passing to the dual picture of the outer billiards map, which is introduced and is strongly utilized in [16]. In this dual picture, we reflect the polygon P at the vertex of tangency rather than reflecting the point. Therefore, the point is held fixed and we look at the sequence of reflected polygons. Figure 4.3 illustrates this. We can easily go back and forth to the dual and come back to the original picture by applying appropriate translations.

In the dual picture, a point is periodic if and only if P comes back to its original position after a finite number of reflections. For a concrete example, see Figure 4.4.

Theorem 13. *Let Q be a periodic domain with respect to polygon P . Then we look at the dual picture where we reflect P instead of points in Q . Pick any point p in P and consider the images of p under these series of reflections, $p = p_0, p_1, \dots, p_n = p_0$, where n is the period of Q which we can assume to be even. Then Q is stable under small variation on λ near 1 if and only if the barycenter $\sum p_i/n$ lies in the interior of Q .*

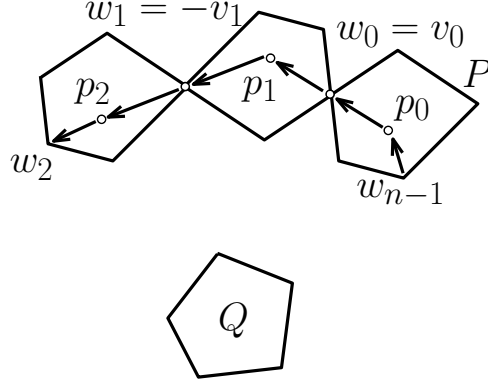


FIGURE 4.3. The dual picture: periodic domain Q is “looking at” P and its reflected images

Proof. We consider the periodic combinatorics $\{v_i\}$ of the domain Q , and given λ , we have the hypothetical periodic point in Q given by the formula

$$q(\lambda) = \frac{1 - (-\lambda)}{1 - (-\lambda)^n} \left(\sum_{i=0}^{n-1} (-\lambda)^{n-1-i} v_i \right)$$

where the choice of the origin is arbitrary and v_i are really the vectors from the origin pointing to the i th vertex of reflection. What we want to conclude is that $\lim_{\lambda \rightarrow 1} q(\lambda) \in \text{int}Q$, because then by continuity we know there exists some $\epsilon > 0$ such that for $\lambda > 1 - \epsilon$, all the iterates $T^j q(\lambda)$ ($0 \leq j < n$) are contained respectively in $T^j Q$, which means that these n points constitute a honest T_λ -periodic orbit. We go to the dual picture as in figure , and pick a point p_0 in the interior of P which we consider as the origin. Then the vector starting from p_0 and ending at the first vertex of reflection is precisely v_0 . In general, if we set w_i to be the vector starting from the point p_i and ending at the $i + 1$ th vertex of reflection then $w_i = (-1)^i v_i$. Since Q is a periodic domain we have $\sum_{i=0}^{n-1} w_i = 0$ or $\sum_{i=0}^{n-1} (-1)^{n-1-i} v_i = 0$. Hence we can use L'Hospital's rule to obtain

$$\lim_{\lambda \rightarrow 1} q(\lambda) = \frac{2}{-n} \left(\sum_{i=0}^{n-1} (n-1-i)(-1)(-1)^{n-i} v_i \right) = \frac{2}{n} \left(\sum_i (n-1-i) w_i \right)$$

since n is even. That is, we are asking whether $\frac{2}{n}(\sum_i (n-1-i)w_i) \in \text{int}Q$. If we put the origin somewhere else, the point p_0 is now seen as a vector and we are asking whether $V_0 = p_0 + \frac{2}{n}(\sum_i (n-1-i)w_i) \in \text{int}Q$ or not. We could have started from the T -translates of Q ; then we will be asking whether $V_j = p_j + \frac{2}{n}(\sum_i (n-1-i)w_{i+j}) \in \text{int}Q$ because the combinatorics will also shift by j . We claim that this destination point is independent on j . We have

$$V_1 - V_0 = p_1 - p_0 + \frac{2}{n} \left(\sum_i (n-1-i)w_i - \sum_i (n-1-i)w_{i+1} \right) = p_1 - p_0 + \frac{2}{n} \left(\sum_{i=1}^{n-1} w_i - (n-1)w_0 \right)$$

but since $\sum_i w_i = 0$, this difference is equal to

$$p_1 - p_0 + \frac{2}{n}(-nw_0) = p_1 - p_0 - 2w_0 = 0.$$

This argument works for other j as well; now we set

$$V = \frac{1}{n} \sum_j V_j = \frac{1}{n} \left(\sum_j p_j + \sum_j \sum_i \frac{2}{n} (n-1-i) w_{i+j} \right)$$

and by interchanging the summation, we finally obtain

$$V = \frac{1}{n} \left(\sum_j p_j + \sum_i \frac{2}{n} ((n-1-i) (\sum_j w_{i+j})) \right) = \frac{1}{n} \left(\sum_j p_j \right).$$

□

We say that a periodic domain Q is symmetric if there exists some affine transformation such that the necklace formed by P and its reflected images according to the combinatorics of Q around Q has a m -fold rotational symmetry around some point in the plane.

Then it turns out that this point of symmetry is contained in the interior of Q , proving Q is stable. Since periodic domains with odd period has 2-fold rotational symmetry, they are also stable. We summarize it as a corollary.

Corollary 14. *All odd periodic domains and symmetric domains are stable.*

Proof. In the dual picture, pick a point q in the interior of Q . Apply $2\pi/m$ rotations $m - 1$ times which would leave the P -necklace invariant. The point q draws a regular m -gon, which is completely contained in Q by symmetry. Therefore, the center of this regular m -gon which equals the barycenter $\sum p_i/n$ is contained in the interior of Q . \square

Corollary 15. *For $n = 3, 4, 5, 6,$ and $8,$ all T -periodic domains outside the regular n -gon are stable.*

Proof. We have already seen this phenomenon for $n = 3, 4,$ and 6 . For $n = 5$, it is implicit in Tabachnikov’s work [16] that the union of all the T -iterates of a periodic tile have a 5-fold rotational symmetry. Regarding the regular octagon, we refer to [14]. \square

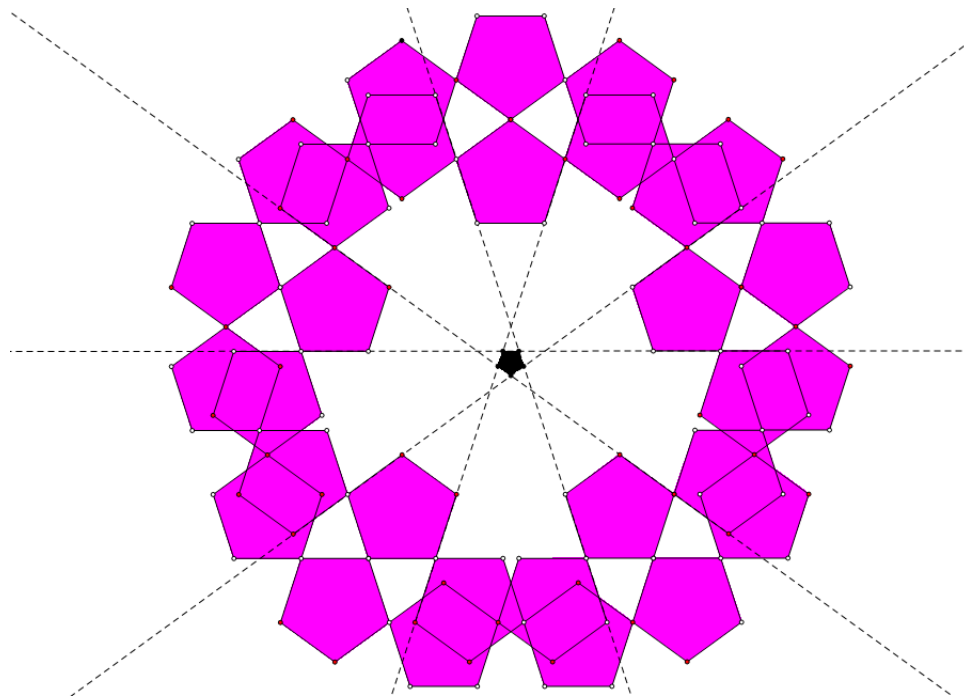


FIGURE 4.4. Dual picture for the 30 periodic orbit outside the regular pentagon; notice how small the periodic tile is relative to P

Above corollary makes it possible for us to conclude that when n is one of above five numbers, then the number of periodic orbits for T_λ outside the regular n -gon diverges as $\lambda \rightarrow 1^-$. It would be nice if we could conclude this for all polygons P . With respect to the standard outer billiards, there is Culter’s theorem which states that there exist infinitely many periodic orbits outside any polygon [20]. We couldn’t find an easy reason why Culter’s periodic orbits should be stable. At the very least, we can prove the following:

Corollary 16. *When P is either a regular polygon or centrally symmetric, the number of T_λ -periodic orbits diverges as $\lambda \rightarrow 1^-$.*

Proof. When P is centrally symmetric, Culter’s periodic orbits have 2-fold symmetry. Moreover, a regular ‘ n -gon for n even is centrally symmetric. Finally, a regular n -gon for n odd has infinitely many periodic orbits of odd period formed by regular $2n$ -gons (easy exercise). \square

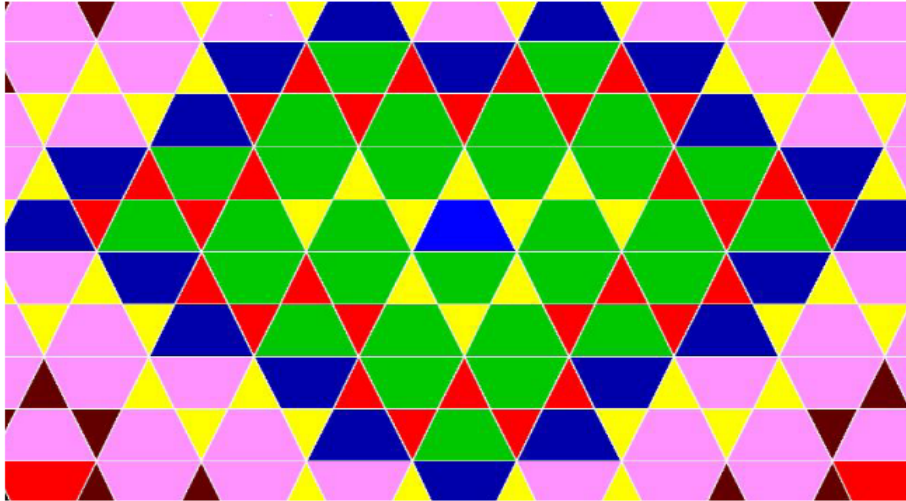


FIGURE 4.5. Dynamics of the outer billiards map outside the trapezoid $P(1/2)$

4.3. Stable Degenerate Periodic Orbits in Trapezoids. In this subsection, we study an interesting class of T_λ -periodic orbits which we call stable degenerate periodic orbits (SDPs) and we show that infinitely many of them exist in trapezoids as $\lambda \rightarrow 1^-$. It is the geometry of the trapezoid that makes it possible to admit such periodic orbits. We call a degenerate T -periodic orbit stable if and only if for λ close enough to 1, it gives rise to an attracting T_λ -periodic orbit (regular or degenerate).

Dynamics of the outer billiards map outside a trapezoid is not too hard to analyze, and it was a part of D. Genin’s thesis [4] under S. Tabachnikov. Our analysis will be similar to his, but also similar to what R. Schwartz had named “pinwheel dynamics” in [15].

Studying stability of degenerate T -periodic orbits is somewhat similar in spirit to Schwartz’s analysis for 2-3-6 triangle [12]. To show that a *near* 2-3-6 triangle does not have a *short* periodic orbit, he analyzes degenerate periodic orbits of the 2-3-6 triangle and show their unstability under perturbation of angles.

Here is the main result of this subsection, from which we can deduce divergence of the number of periodic orbits without knowing the stability of Culter’s periodic orbits.

Theorem 17. *Any trapezoid has infinitely many stable degenerate periodic orbits (SDPs).*

Corollary 18. *For any trapezoid, the number of T_λ -periodic orbits diverges as $\lambda \rightarrow 1^-$.*

We expect that an analogue of Theorem 17 to be true for a large class of polygons, especially for polygons having parallel sides.

Up to affine transformations of the plane and renaming the vertices cyclically, the set of all quadrilaterals are parametrized by a single variable with range $0 < \alpha < 1$. We use the notation $P(\alpha)$ to describe the quadrilateral with vertices $D = (1/2, -1/2)$, $C = (1/2, \alpha/2)$, $B = (-1/2, \alpha/2)$, and $A = (-1/2, -1/2)$. Therefore, $P(\alpha)$ is lattice if and only if α is rational. And it is well-known that (first proved in [6]) if a polygon is lattice, every point is T -periodic. See Figure 4.5 which verifies this. Among all trapezoids, the one with $\alpha = 1/2$ is the simplest, since it is either described as a half-regular hexagon or a union of three equilateral triangles. We would like to introduce an ambitious conjecture to motivate the interested readers.

Conjecture 19 (3-5-7 Conjecture). *All T_λ -periodic orbits for $P(1/2)$, for $0 < \lambda < 1$, fall into one of three categories:*

- i) The unique Fagnano periodic orbit (period 4)
- ii) Regular T -periodic orbits (period multiples of 10)
- iii) Stable degenerate T -periodic orbits, whose periods bijectively correspond with the set of all positive natural numbers congruent to 3, 5, or 7 mod 10.

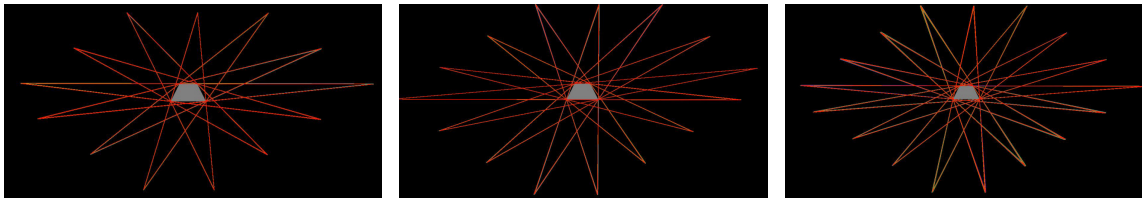


FIGURE 4.6. 13, 15, 17 periodic orbits for the trapezoid $P(1/2)$

This conjecture has finiteness (with very explicit numbers) of T_λ -periodic orbits for all $0 < \lambda < 1$ as a corollary for $P(1/2)$, simply because with any contraction, we have only finitely many of type ii) and iii) periodic orbits in a bounded ball. Interestingly, for each number ending with either 3, 5, or 7, there exists a unique SDP having that number as its period. This existence is not hard, and will be proved shortly. Analogues of this conjecture exist for all other lattice trapezoids.

Let q be a point lying on the singular rays S in some degenerate periodic orbit. The ray S divides the neighbor into two regions, say U and V . When we define Tq using the rule of T on U , let us say that q follows U .

Proposition 20 (Stability Criterion). *Let $\mathcal{O} = \{q_i\}_{1 \leq i \leq k}$ be a degenerate T -periodic orbit. Then \mathcal{O} to be stable if and only if for each $q \in \mathcal{O} \cap S$, the vector $-q'(1)$ (negative of the derivative of the limit curve at $\lambda = 1$) points toward the continuity region that it follows.*

We illustrate this by an example. In Figure 4.7, three points P , Q , and R form a degenerate periodic orbit. Since P is the only point in S , to show that this orbit is stable we only need to show that the derivative of the limit curve for P points upward at $\lambda = 1$. In this special case this is clear since this periodic orbit is the Fagnano orbit around the triangle ADC . When we slightly decrease λ , three points rotate clockwise around the affine-center of the triangle ADC .

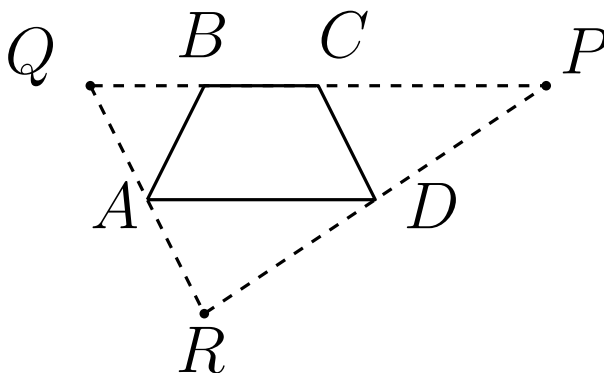


FIGURE 4.7. An example of SDP

4.3.1. *Case Study of $P(1/2)$.* In this section, we focus on the special trapezoid $P(1/2)$. All the essential ingredients in the proof of Theorem 17 is contained in this case study, so that a reader can skip the proof for the general case.

Proposition 21 (3-5-7 Conjecture, weak form). *For any positive integer congruent to either 3, 5, or 7 (mod 10), there exists a SDP with that number as its period. Moreover, there are no more SDPs.*

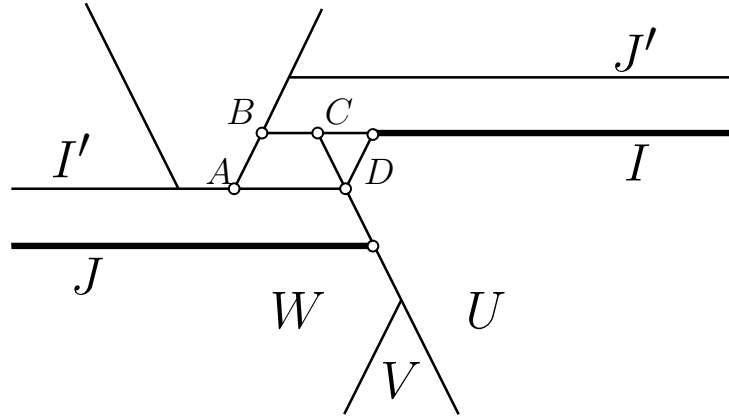


FIGURE 4.8. Continuity regions for T^2

Proof. We consider the map T^2 rather than T itself. Then depending on in which region you are in (regions are drawn in Figure 4.8), the map T^2 is just the addition by an appropriate vector. To be more specific, inside the region U , T^2 is addition by the vector $2 \cdot \overrightarrow{CA} = u$, and inside the regions V and W it is addition by vectors $2 \cdot \overrightarrow{DA} = v$ and $2 \cdot \overrightarrow{DB} = w$ respectively.

A degenerate periodic orbit must contain a point on S . Let us assume that it contains a point on the singular ray extending the edge BC . We ignore a short initial segment and consider the ray I as in Figure 4.8 so that below I , T^2 is addition of v . On I , we make an artificial choice of following the rules of U . (We prove later that the other choice will not give stable periodic orbits) Then it is easy to see that any point starting on I goes to a point in J under some iterates of T^2 , because the vectors u, v, w change the y -coordinate by $+2, 0, -2$. Compose this map $\Psi : I \rightarrow J$ with rotation of J by π with respect to the point D to obtain a self-map $\Phi : I \rightarrow I$. Note that Φ is an interval exchange transform except it flips each interval, because the map $I \rightarrow J$ is a bijective piecewise translation. Apparently, Φ is not defined on a discrete set of points.

We claim that a fixed point of Φ gives a SDP with odd period. Assume $x \in I$ is a fixed point. Then under T^{2k} for $k \geq 1$, we have $T^{2k}x \in J$ such that $T(T^{2k}x) = x$. So x gives a periodic orbit with period $2k + 1$, and we defer the proof of stability.

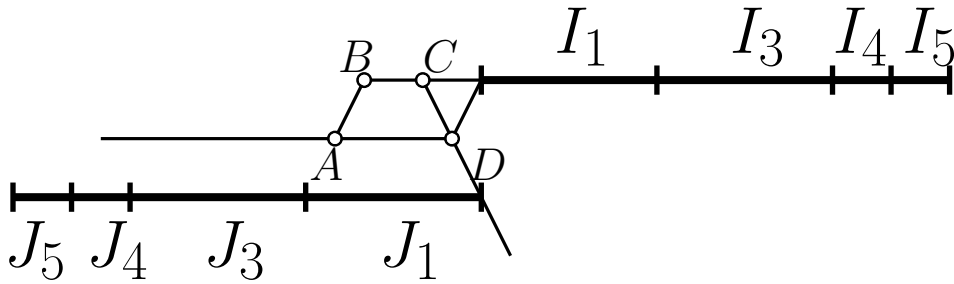


FIGURE 4.9. An interval exchange transform

Figure 4.9 shows the map Φ . In this figure, I_k denote the segment in I that is mapped to J_k under T^{2k} . Our convention was that $A = (-1/2, -1/2)$, $D = (1/2, -1/2)$ so that $|AD| = 1$ and with this scale, the map $I \rightarrow J$ has period 4, so that we only need to look at intervals I_1, I_3, I_4 , and I_5 whose lengths add up to 4. We also defer the proof of periodicity. So clearly, Φ has precisely two fixed points in this region, one in I_1 and the other in I_3 . They give rise to periodic orbits of period 3 and 7, respectively.

It is easy to check that if we go for one period of Φ , the index k increases by 5 so that we obtain periodic orbits of T whose period is larger by 10 than the corresponding previous one. Therefore, we obtain $10t + 3$ and

$10t + 7$ SDPs for all $t \geq 0$. We can repeat the same analysis for another pair of singular rays I' and J' to obtain $10t + 5$ SDPs for $t \geq 0$.

We only sketch the proof of the second statement, because it is tedious. It is enough to show that all SDPs come from fixed points of Φ or $\Phi' : I' \rightarrow I'$. We need to deal with three things: first is what happens when we make the other choice on I (or on I'). It will be shown later that no matter what choice we make on I , under slight decrease on λ , the limit curve will flow downwards, contradicting the stability. In the same way, we can show that on J , we really have a unique choice of T^2 for the degenerate periodic orbit to be stable. Next, assume x is a periodic point of Φ . Then it repeats the same combinatorics several times depending on its Φ -period. This cannot be a combinatorics for a regular T_λ -periodic orbit because with contraction, we never have “periodic” combinatorics. Finally, we prove by explicit computation that the other two pairs of singular rays (ones extending segments CD and AB) do not give rise to SDPs. We also need to deal with ignored initial segments of I and I' . This concludes the proof. \square

4.3.2. *General Trapezoids.* We do not prove the following lemma (used in the proof of Proposition 21) as it was covered in [5].

Lemma 22. *For $\alpha = p/q$, the map Φ has period $2q$.*

Therefore, for any lattice trapezoid we have an analogue of Proposition 21: SDPs come in families such that the periods of each family forms an arithmetic progression. The size of the gap in these arithmetic progressions are the same for a given lattice trapezoid, and the formula for the size should have a simple expression in terms of p and q . For example, one can deduce that in the trapezoid $P(1/n)$, we get arithmetic progressions of gap $2(2n + 1)$.

Now we proceed to prove the stability lemma.

Lemma 23. *For all trapezoids, any degenerate periodic orbit coming from a fixed point of Φ (or Φ') is stable.*

Proof. Recall the formula for the limit curve for the combinatorics $\{v_i\}_{i=0}^{n-1}$:

$$q(\lambda) = \frac{\sum_{i=0}^{n-1} (-\lambda)^i v_i}{\sum_{i=0}^{n-1} (-\lambda)^i}.$$

What we only need to show is that $p'(\lambda)$ has positive y -component, because it implies that if we decrease λ slightly from 1, the limit curve is contained in the interior of U , thereby giving a regular T_λ -periodic orbit.

By an explicit computation, one can show that

$$(4.1) \quad q'(\lambda) = \frac{1}{K^2} \sum_{i=0}^{n-1} (-1)^i (k - i) v_i$$

where $K = \sum_{i=0}^{n-1} (-\lambda)^i$.

Let x be a fixed point for Φ . If we inspect the “itinerary” of x under T , it has the form $au + bv + (a - 1)w$ followed by the reflection with respect to the vertex D , where $a \geq 1$ and $b \geq 0$ are integers. Vectors u, v, w correspond to combinatorics CA, DA , and DB , respectively. Therefore, from this information we can compute the sum in Equation 4.1 explicitly to obtain

$$q'(\lambda) = \frac{1}{K^2} \{(a^2 + ab)(C - D) + (ab - b + a^2 - a)(B - A)\}.$$

For any a and b , coefficients for $C - D$ and $B - A$ are positive, so we are done. Notice that above formula is a projective invariant (and it should be), a fact not clear from Equation 4.1. \square

Remark 24. Consider the aforementioned case where we make the other choice on the singular ray I to obtain a modified combinatorics $\hat{u} + (a - 1)u + bv + (a - 1)w$ (followed by a reflection on D). We immediately see from above calculation that the derivative of the limit curve still point upward, showing that this choice is never stable.

Now we have all the ingredients to conclude Theorem 17.

Proof of Theorem 17. Let Q be the initial point of the ray J , and let P be the preimage of Q under T^2 . If we forget about the flip in the orientation, the map Φ is the left shift by 1. Consider the decomposition of the ray I starting from the point P by disjoint union of intervals I_k where the interior of I_k has T^2 -period of k to get to J . Since Φ is a shift composed with piecewise flips on I_k , the interval I_k will contain a fixed point of Φ if $|I_k| > 1$.

Let K and L be rays separating regions U and V , V and W , respectively. Then discontinuities of Φ come precisely from intersections of K and L with a family of horizontal lines $y = -2t - 3/2$, $t \geq 0$. So when we pick a point H on I having distance $d \gg 1$ from P , we see that the number of discontinuity points contained in the segment PH is asymptotically d , but it never exceeds d .

In the case where α is rational, we can explicitly see that the interval I_3 containing P as its left endpoint has length greater than 1, so by periodicity we have infinitely many intervals of length greater than 1, concluding the proof. In the irrational case, the lengths of intervals I_k for $k \geq N$ can never be all the same for any N , so we have infinitely many intervals of length greater than 1. \square

4.4. Star Shaped Periodic Orbits in Regular Polygons. Recall that regular polygons have the following nice property: For all $0 < \lambda < 1$, there exists a regular periodic orbit (namely, the Fagnano orbit) which attracts the whole domain for λ small. In this subsection, we figure out what is the precise threshold value of λ such that the Fagnano orbit is the unique attracting periodic orbit. Let us call this λ_2 , as this is precisely when the second periodic orbit appears. It will follow that for all regular polygons, this second periodic orbit will exist for all $\lambda_2 < \lambda < 1$ and so we can define λ_3 to be the threshold value of λ when the third periodic orbit appears as well.

It turns out that the second periodic orbit, for $n \geq 5$, is rotationally symmetric and skips every other vertex (Figure 4.12). Therefore, for $n \geq 5$ and odd, it will have period n and otherwise it will have period $n/2$. Let us label the vertices of the regular n -gon by v_1, \dots, v_n counterclockwise. Then we say a T_λ -periodic orbit \mathcal{O} is star shaped (with gap k) if its combinatorics has the form $\{v_1, v_{1+k}, v_{1+2k}, \dots, v_1\}$. The star shaped periodic orbit of gap k (unique up to rotation around the center) exists if and only if $n \geq 2k + 1$. Apparently, these orbits all come from T -periodic orbits, and once they start to exist for some λ , it persists as λ increases to 1.

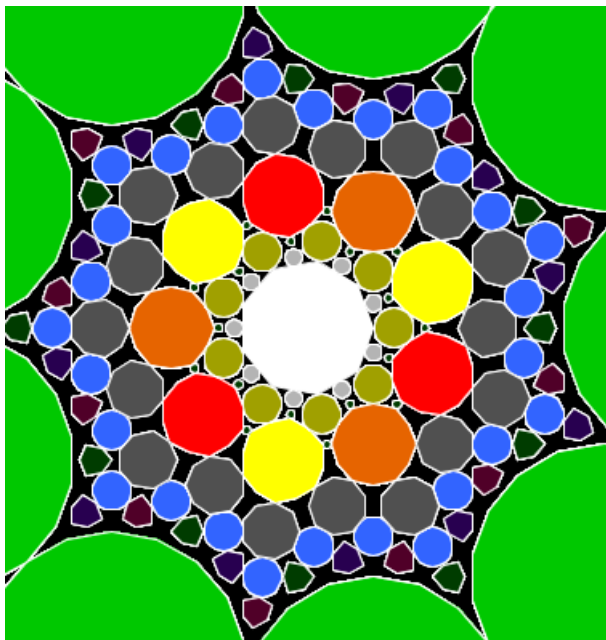


FIGURE 4.10. In the regular nonagon, one sees four star shaped orbits

We have tabulated some values of λ_2 and λ_3 below, up to three decimal points. Note that for the regular pentagon, λ_2 equals the golden ratio. It is a fun exercise to prove this by hand.

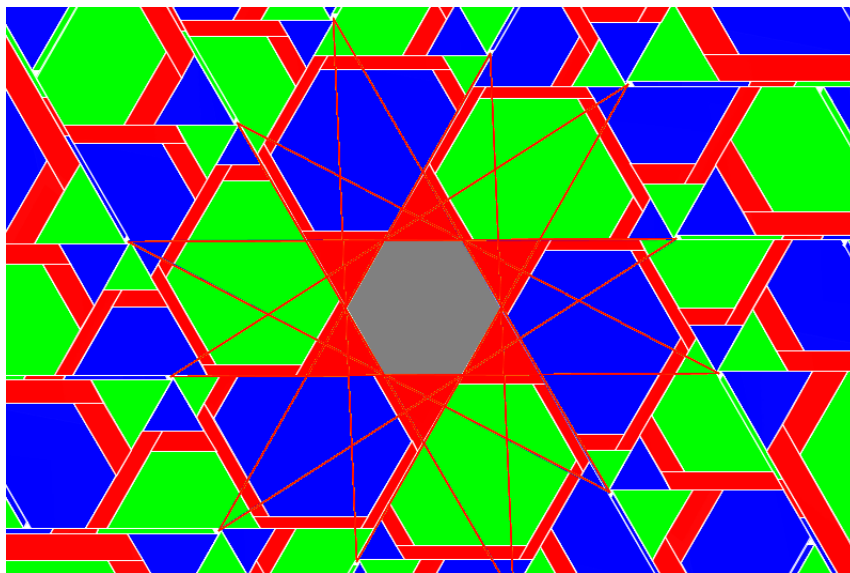


FIGURE 4.11. Appearance of the third (or the fourth, depending on how you count multiplicities) periodic orbit for the regular hexagon near $\lambda = 0.878$

n	3	4	5	6	7	...	$n \geq 7$
λ_2	0.890	0.755	0.618	0.500 (a pair)	0.445	...	$1/(1 + 2 \cos(2\pi/n))$
λ_3	0.918	0.890	0.794	0.878	0.802	...	$1/2 \cos(2\pi/n)$ (conjectural)

This fact is a special case of the following result.

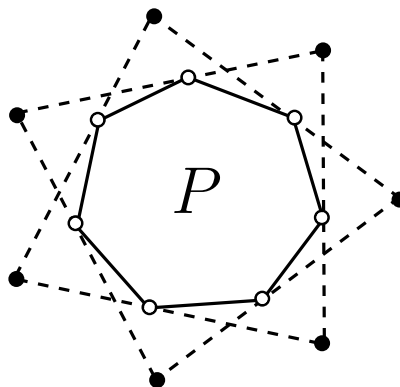


FIGURE 4.12. The star shaped orbit of gap 2 is “revealing” the Fagnano orbit

Theorem 25 (with F. Bozgan). *For regular n -gons ($n \geq 5$), the first threshold λ_2 equals $1/(1 + 2 \cos(2\pi/n))$.*

Proof. See Appendix A. For now, we only mention that while it is easy to establish $\lambda_2 \leq 1/(1 + 2 \cos(2\pi/n))$ (Figure 4.12 almost contains a proof), the other direction is painful. \square

The following is straightforward again:

Proposition 26. *For $n \geq 2k + 1$, we have*

$$\lambda_k \leq \frac{\sin((k - 1)\pi/n)}{\sin((k + 1)\pi/n)}$$

where λ_k is k th threshold for the regular n -gon.

Here is an extension of Theorem 25. The intuition behind this conjecture is that the star shaped periodic orbits are more “stable” than other ones.

Conjecture 27. For $n \geq 2k + 1$, we have

$$\lambda_k = \frac{\sin((k-1)\pi/n)}{\sin((k+1)\pi/n)}.$$

When $k = 2$, we recover the previous proposition. Figure 4.13 is the illustration of this conjecture for $k = 3$. Notice that there exist precisely two periodic orbits, both of which are star shaped. More importantly, notice that two basins of attractions are “tangent” to each other so that if we increase λ slightly, the third periodic orbit comes to life in each case.

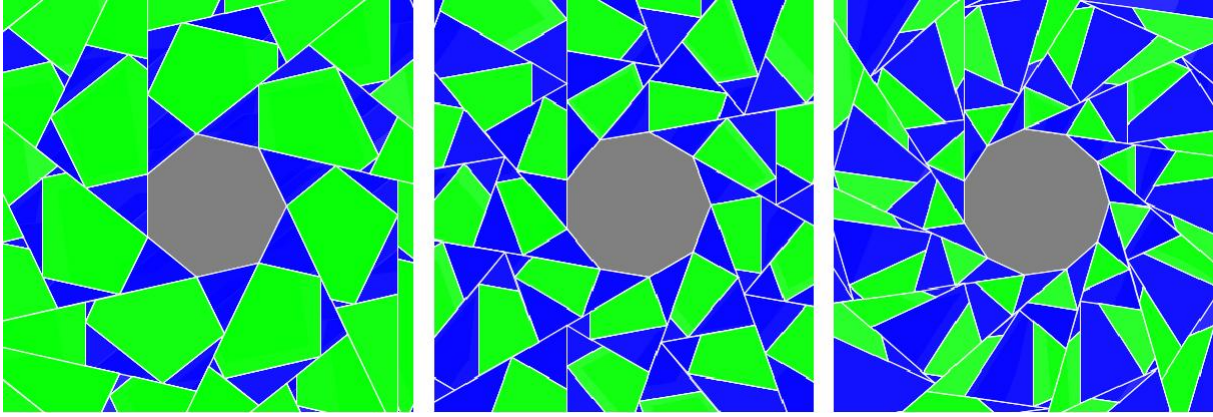


FIGURE 4.13. Illustrations of the higher conjecture $k = 3$

We are quite confident that we can resolve this conjecture, at least for the case $k = 3$, in a finite amount of time. If this conjecture were true, we have $\lim_{n \rightarrow \infty} \lambda_k = (k-1)/(k+1)$ which approaches 1 as $k \rightarrow \infty$.

4.5. Periodic Orbits of Winding Number 1 in Quadrilaterals. In this subsection, we restrict our attention to quadrilaterals, and look at periodic orbits of *winding number* 1. Given a periodic point p (either with respect to T or T_λ), we can define its winding number by the number of times p has wrapped around P until it returns to its position. By analyzing periodic orbits of winding number 1, we will see that for every convex quadrilateral, there exists an attracting T_λ -periodic orbit possibly except for one value of λ . (Proposition 28)

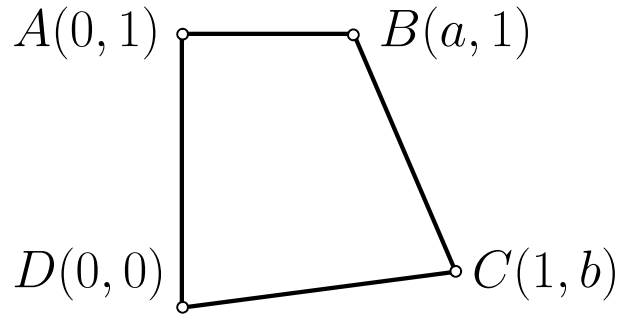


FIGURE 4.14. Quadrilateral (a, b)

Up to affine transformations, any convex quadrilateral can be represented by a pair of reals (a, b) where $0 < a$, $b < 1$, and $ab < 1$. This pair represents the quadrilateral with vertices $A = (0, 1)$, $B = (a, 1)$, $C = (1, b)$, and $D = (0, 0)$, as in Figure 4.14. This choice of parameters will turn out to be convenient in Section 5. Moreover, we

can cyclically rename the vertices; the permutation $(A, B, C, D) \rightarrow (D, A, B, C)$ correspond to the transformation $(a, b) \mapsto (1 - b, (1 - 1/a)/(1 - b))$ and one can easily check from this that we can further assume $0 < a < 1$ and $0 < b < 1$ without loss of generality.

Proposition 28. *For every convex quadrilateral, there exists a unique attracting periodic orbit of winding number 1 possibly except for one value of λ .*

- (1) *If $a + b \leq 1$: The unique attracting periodic orbit of winding number 1 exists for $\lambda \in (0, 1) \setminus \{1 - b\}$ and is*
 - (a) *the Fagnano orbit in $\lambda \in (0, a)$*
 - (b) *the (degenerate) Fagnano orbit at $\lambda = a$*
 - (c) *the triangular periodic orbit skipping the vertex A in $\lambda \in (a, 1 - b)$,*
 - (d) *the triangular periodic orbit skipping the vertex B in $\lambda \in (1 - b, 1)$.*
- (2) *If $a + b > 1$: The unique attracting periodic orbit of winding number 1 exists for all $\lambda \in (0, 1)$ and is*
 - (a) *the Fagnano orbit in $\lambda \in (0, a)$*
 - (b) *the (degenerate) Fagnano orbit at $\lambda = a$*
 - (c) *the triangular periodic orbit skipping the vertex A in $\lambda \in (a, 1)$.*

Proof. Given (P, λ) , there are only five possible periodic orbits of winding number 1. Using Equation 2.1, we can solve for the condition for each of them to exist. □

One should note that if $a + b \leq 1$, in the range $\lambda \in (a, 1) \setminus \{1 - b\}$, the unique regular period 3 orbit with winding number 1 has the neighborhood of the singular ray extending the side AB as a basin of attraction. At the critical value $\lambda = 1 - b$, however, we get two degenerate “triangular” periodic orbits, both of which are non-attracting according to an observation made in the beginning. Then what happens to the points around the singular ray at this value of λ ? Therefore, we expect to observe interesting behavior near the singular ray at this value of λ . Such a behavior is already visible in Figure 4.15, and it will be analyzed in the next section.

What is also very interesting is that the behavior of the map near the critical value λ . Depending on the quadrilateral, a whole variety of phenomena can happen. We did not even attempt to enumerate all possibilities, since there are too many. However, what is common in all cases is that as λ passes through the critical value $1 - b$, there is a abrupt change in the picture, and this value deserves the name bifurcation value.

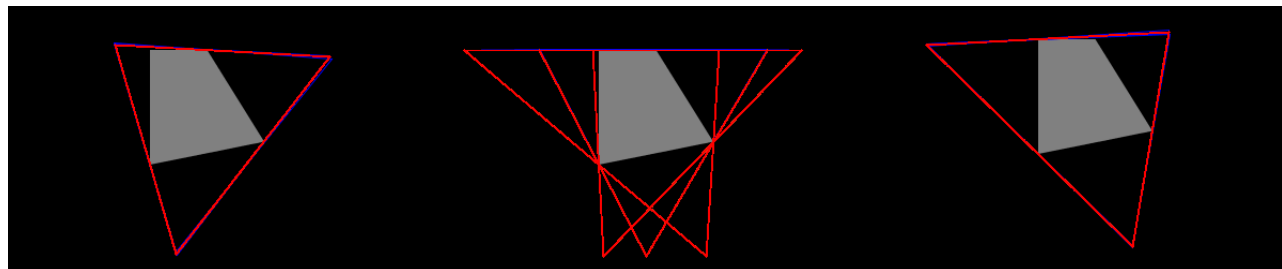


FIGURE 4.15. Attracting periodic orbits for $P = (0.5, 0.2)$ when $\lambda = 0.75, 0.8, 0.85$ (from left to right)

From next section, we will see that generically, there exists a degenerate attracting periodic orbit at $\lambda = 1 - b$, whose period can be arbitrarily high. Interestingly, it can be either “transient” or stable under decreasing λ . To illustrate the first possibility, we consider the quadrilateral $P = (0.5, 0.2)$ and look at its behavior right before 0.8, at 0.8, and right after 0.8. The conclusion is that for $a = 0.5 < \lambda < 0.8 = 1 - b$, every point is attracted to the triangular orbit skipping the vertex A . Similarly, when λ is slightly larger than 0.8, (at least up to 0.85) every point is attracted to the triangular orbit skipping the vertex B . At the bifurcation value $\lambda = 0.8$, we suddenly see a degenerate periodic orbit of period 10 (one of the ten points lies in the middle of the edge AB) which again attracts the whole domain. See Figure 4.15.

But now let us consider the quadrilateral $P = (0.1, 0.7)$ (Figure 4.16). Before the bifurcation, it has four attracting periodic orbits, whose basins of attraction are colored by red, green, blue (hard to see), and white (even harder to see). The blue one corresponds to the triangular periodic orbit which attracts barely anything in this case. The periodic orbit corresponding to the red region becomes the attracting degenerate periodic orbit

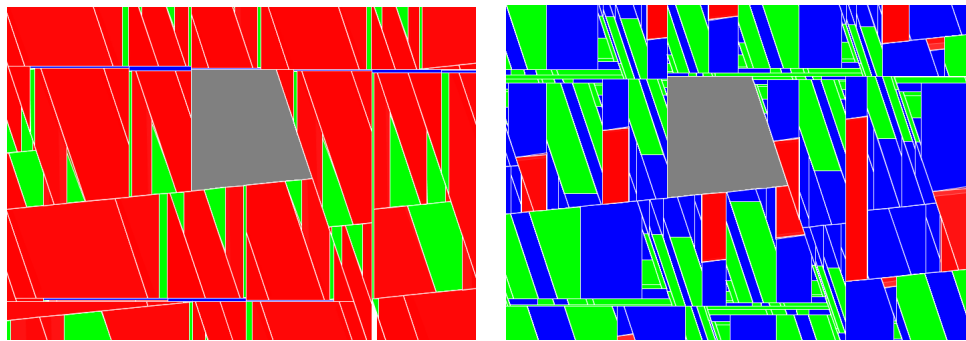


FIGURE 4.16. Basins of attraction for $P = (0.1, 0.7)$ when $\lambda = 0.79, 0.81$ (left, right)

at the bifurcation value. After the bifurcation, however, we see only three periodic orbits, and interestingly none of them corresponds to any of the four periodic orbits (in terms of combinatorics) that existed right before bifurcation.

Finally, let us look at one more case when $P = (0.15, 0.75)$ described in Figure 4.17. Now around the bifurcation value, we always see two periodic orbits, and again they are disjoint from each other. In all cases, the green region correspond to a triangular periodic orbit. Again, the degenerate attracting periodic orbit which exists at $\lambda = 0.85$ is stable under decreasing λ , and we have included one more picture (the leftmost one) to convince you that this periodic orbit appears “all of a sudden” and attracts most of the domain. This shows a striking contrast to the square case from Section 3, in which whenever a new periodic orbit appears, its basin of attraction grows steadily starting from a point.

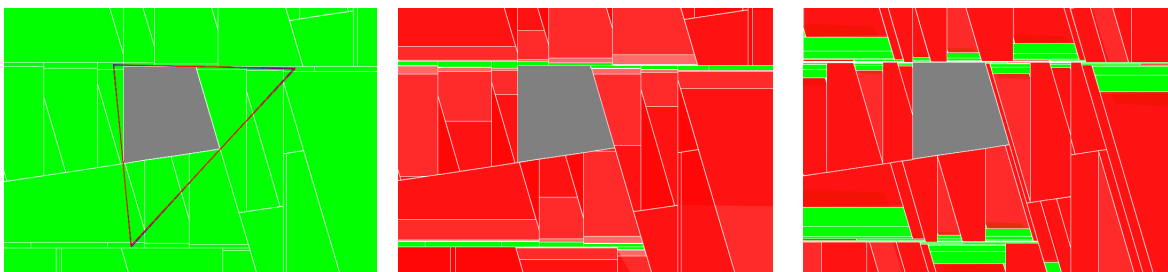


FIGURE 4.17. Basins of attraction for $P = (0.15, 0.75)$ when $\lambda = 0.8345573775, 0.8345573800,$ and 0.851 (from left to right) In the leftmost picture, the whole domain is attracted to the triangular orbit. But after some threshold value of λ which apparently lies between 0.8345573775 and 0.8345573800 , most of the domain gets attracted to a periodic orbit of very high period “all of a sudden.” (red region in the second picture)

Some experiments with pentagons reveal that they can possess multiple periodic orbits of winding number 1. However, the following conjecture seems true.

Conjecture 29. *Given any convex polygon P , it has an attracting periodic orbit of winding number 1 possibly except for finitely many values of λ .*

5. ANALYSIS OF THE TRIANGULAR TRANSITION

5.1. Preview. In this section, we analyze the “triangular transition” observed in Subsection 4.5: for quadrilaterals (a, b) with $a + b \leq 1$, when $\lambda = 1 - b$, we have a transition between two triangular periodic orbits. Hence in this section, it is assumed that $\lambda = 1 - b$ always, (given a quadrilateral) and we study the dynamics near the singular ray \overrightarrow{AB} (Figure 4.14).

Near the singular ray \overrightarrow{AB} , it turns out that every point either converges to a degenerate periodic orbit or to a Cantor set, depending on the quadrilateral (a, b) . Moreover, this is precisely determined by whether the rotation number of a certain map $g_{a,b}$ is rational or irrational. From this, we can say that for some open and dense set of quadrilaterals (satisfying $a + b \leq 1$), all the points converge to a degenerate periodic orbit.

To outline the proof, we restrict our attention to the region $L(\epsilon)$ (Figure 5.1) which is forward invariant under dynamics of T_λ . This thin neighborhood is divided into “above” and “below” from which we deduce that the dynamics of T_λ is reduced to studying two return maps which are 1-dimensional piecewise contractions. (Lemma 30) We show that the rotation numbers of these maps are well-defined and vary continuously with the parameter. (Lemma 32) If this rotation number is irrational, then there must be an attracting Cantor set. We show this existence by showing that the rotation number is non-constant as a function of the parameter by computing 2 examples. (Theorem 34)

Therefore, the key theoretical tool is the theory of rotation number for 1-dimensional maps that are not necessarily continuous. Such a theory was developed in [11, 10, 1], and we summarize it in Appendix B. In the following two subsections, we carry out the above outline and conclude the theorem. In the last subsection, we analyze the complementary case of rational rotation number and deduce existence of attracting periodic orbits. We note that the 1-dimensional return maps appearing in our analysis are piecewise increasing contractions on 2 intervals, which were studied in [3, 21].

5.2. Attracting Cantor Sets . In this subsection, we deduce that there exist attracting Cantor sets. From now on, $a + b \leq 1$ is always assumed. For simplicity, let us set $\mu = 1/\lambda = 1/(1 - b)$. We start by restricting our attention to an invariant set. In Figure 5.1, the point E of \overline{EA} is defined to satisfy $T_\lambda^2 E = B$. A computation yields $E = (-\mu - (1 - a)\mu^2, 1)$.

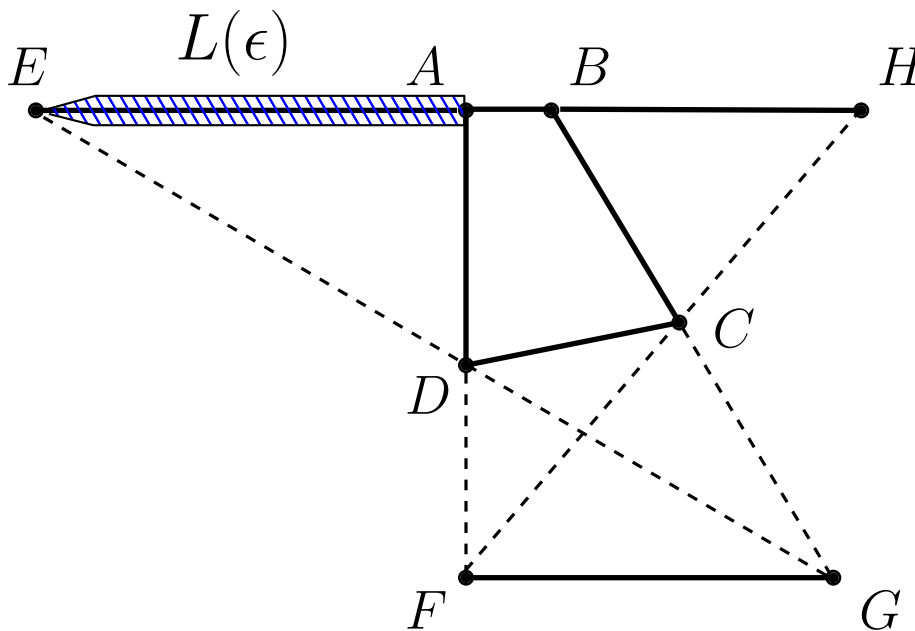


FIGURE 5.1. Forward invariant set $L(\epsilon)$

Lemma 30. *Assume $a < 1 + \lambda - \lambda^3 - \lambda^4$. Then for sufficiently small $\epsilon > 0$, the ϵ neighborhood $L(\epsilon)$ of the line segment $L = (-\mu - (1 - a)\mu^2, 0) \times \{1\} = \overline{EA}$ is forward invariant under iterates of T_λ . That is, for any $p \in L(\epsilon)$, there exists the smallest $n > 0$ such that $T_\lambda^n p \in L(\epsilon)$. Moreover, $\text{dist}(T_\lambda^n p, L) \leq \lambda^3 \text{dist}(p, L)$ so that the sequence y -coordinates of the iterates of the first-return map to $L(\epsilon)$ converges exponentially to the y -coordinate of L .*

To be completely rigorous, we need to take a neighborhood which is “sharp” near E .

Proof. Under T_λ^2 , $L(\epsilon)$ is mapped to a $\lambda^2\epsilon$ -neighborhood of the line segment \overline{BH} . Let us denote the part of $T_\lambda^2 L(\epsilon)$ lying above \overline{BH} by U^+ and the opposite by U^- . Points in U^- , either by T_λ or by T_λ^2 , end up in $L(\epsilon)$ for all $(a, b) \in X$. For all the points in U^+ to be contained in $L(\epsilon)$ after T_λ , we require $|\overline{AH}| \times \lambda < |\overline{EA}|$, which is equivalent to $a < 1 + \lambda - \lambda^3 - \lambda^4$.

Now the last statement is clear, since a point $p \in L(\epsilon)$ comes back to $L(\epsilon)$ either by T_λ^3 or T_λ^4 and hence the y -coordinate relative to L gets contracted either by λ^3 or λ^4 each time. \square

From now on, we will denote X to be the set of quadrilaterals (a, b) (with $a + b \leq 1$) satisfying the inequality $a < 1 + \lambda - \lambda^3 - \lambda^4$, and we will restrict our attention to quadrilaterals in X . This set is convex, and it corresponds to the colored region in Figure 5.3. The left border represents the curve $a = 1 + \lambda - \lambda^3 - \lambda^4$.

In the invariant region $L(\epsilon)$, the dynamics is “trivial” in the y -coordinate, so we can treat $L(\epsilon)$ as a disjoint union of two line segments (or “infinitesimally thin” rectangles) which we denote by L^+ and L^- , each having the same length with L . That is, to study the forward orbit of a point in $L(\epsilon)$, we only need to keep track of x -coordinates and relative position to L (either above or below) of its iterates. Hence, the dynamics is reduced to two 1-dimensional ones, which are the first-return maps to L^+ and L^- . Let us call them f and g , respectively; they are certainly piecewise affine contractions.

For simplicity, we will apply an orientation-preserving affine transformation to send the line L to the unit interval $(0, 1]$ and regard g as a map from the circle S^1 to itself. Then g takes the following form:

Lemma 31. *The first-return map of L^- has the formula*

$$(5.1) \quad g(x) = \begin{cases} \lambda^4(x - 1 + H/L) + 1 & 0 < x < 1 - H/L \\ \lambda^6(x - 1) + (1 - Y/L) & 1 - H/L < x \leq 1 \end{cases}$$

where

$$\begin{aligned} L &= \mu + (1 - a)\mu^2 \\ H &= L - a\mu^3 \\ Y &= \lambda(1 + \lambda)(1 + a\lambda^2 - \lambda^3) \end{aligned}$$

are positive constants.

Proof. Straightforward computation. \square

Lemma 32. *For $(a, b) \in X$, the first-return map to L^- , $g_{a,b} \in \mathcal{S}$ so that its rotation number $\rho(g_{a,b})$ is well-defined mod 1. Moreover, this rotation number is continuous in a and b .*

Proof. For the first statement, we need to check that for $(a, b) \in X$, there is a lift $G_{a,b}$ that is strictly increasing and of degree 1. We simply define

$$G_{a,b}(x) = \begin{cases} g(x) & 0 < x < 1 - H/L \\ g(x) + 1 & 1 - H/L < x \leq 1 \end{cases}$$

on $(0, 1]$ and extend to \mathbb{R} by $G_{a,b}(x + 1) = G_{a,b}(x) + 1$. If $g_{a,b}$ were injective, then $G_{a,b}$ is strictly increasing. But injectivity of $g_{a,b}$ is same as checking $\lim_{h \rightarrow 0^+} g_{a,b}(h) > g_{a,b}(1)$, and the inequality from Lemma 30 implies this one.

Next we argue continuity of the rotation number. Given five parameters $\lambda_1, \lambda_2, c_1, c_2$, and t , which all lie in $(0, 1)$, we can associate the following function:

$$h(x) = \begin{cases} \lambda_1 x + c_1 & 0 < x \leq t \\ \lambda_2 x + c_2 + 1 & t < x \leq 1 \end{cases}.$$

For any $(a, b) \in X$, $G_{a,b}$ takes above form for appropriate parameters. If we fix four parameters and move the remaining one continuously, (the closure of) the filled-graph of h moves continuously in the Hausdorff topology. Therefore, we can move above five parameters simultaneously, and still the filled-graph moves continuously. It is clear that varying a and b continuously moves five parameters continuously. \square

We can similarly show that $f_{a,b}$ is injective and the rotation number $\rho(f_{a,b})$ is well-defined.

Remark 33. Viewed as a circle map, $g_{a,b}$ is not continuous at two points, $1 - H/L$ and $1 (= 0)$. But we have intentionally left $g_{a,b}$ undefined at $1 - H/L$, while at $x = 1$, it is defined to be continuous from the left. Recall that when the rotation number of $g_{a,b}$ is rational, then $\tilde{g}_{a,b}$ has a periodic orbit where $\tilde{g}_{a,b}$ can be different from $g_{a,b}$ at points of discontinuity. At $x = 1$, there is no ambiguity since the portion of the segment L close to the point E is not forward invariant under T_λ ; hence we can assume $\tilde{g}_{a,b}(1) = g_{a,b}(1)$. From now on, when we say “ $g_{a,b}$ -periodic orbit”, it is assumed that $g_{a,b}$ has selected one of two possible values for $g_{a,b}(1 - H/L)$. The same observation applies to $f_{a,b}$.

Theorem 34. *For uncountably many choice of (a,b) , for the map T_λ , there exists a Cantor set K such that $\omega(x) = K$ for all $x \in L(\epsilon)$.*

Proof. This is achieved by showing two things. First, we show that if $\rho(g_{a,b})$ is irrational, then $\omega(x)$ for $x \in L(\epsilon)$ is a Cantor set. Then it only remains to show that this rotation number is non constant in X since it is convex.

To begin with, it is clear that for $x \in L(\epsilon)$, its limit set under outer billiards with contraction $\omega_{T_{1-b}}(x)$ equals the union of $\omega_g(x)$ and $\omega_f(x)$ viewed as subsets of L together with their finitely many T_{1-b} -iterates. Now, if $\rho(g_{a,b})$ is irrational, then $g_{a,b}$ cannot have a periodic orbit. Since a periodic orbit of $f_{a,b}$ would give a periodic orbit for $g_{a,b}$ (will follow from Proposition 36 but easy to check directly), it implies that $\rho(f_{a,b})$ must be irrational as well. Therefore, it follows that $\omega_g(x)$ and $\omega_f(x)$ are both Cantor sets on L . So $\omega_{T_{1-b}}(x)$ is a finite union of Cantor sets. This set lies on a union of two lines, and since it is invariant under a piecewise contraction, it must have one-dimensional Lebesgue measure zero. Therefore, $\omega_{T_{1-b}}(x)$ must be totally disconnected and it is a Cantor set as well.

For the second step, we claim that at $(0.6, 0.2)$, the rotation number is $1/2$: it is a simple computation to check $g_{a,b}^2$ has a fixed point while $g_{a,b}$ does not. On the other hand, at $(0.3, 0.2)$, the rotation number of $g_{a,b}$ is 1 because it has a fixed point. Therefore we are guaranteed uncountably many pairs (a, b) with an irrational rotation number. \square

5.3. Degenerate Periodic Orbits. In this section, we continue the same analysis, but now we will look at the case when g has a rational rotation number.

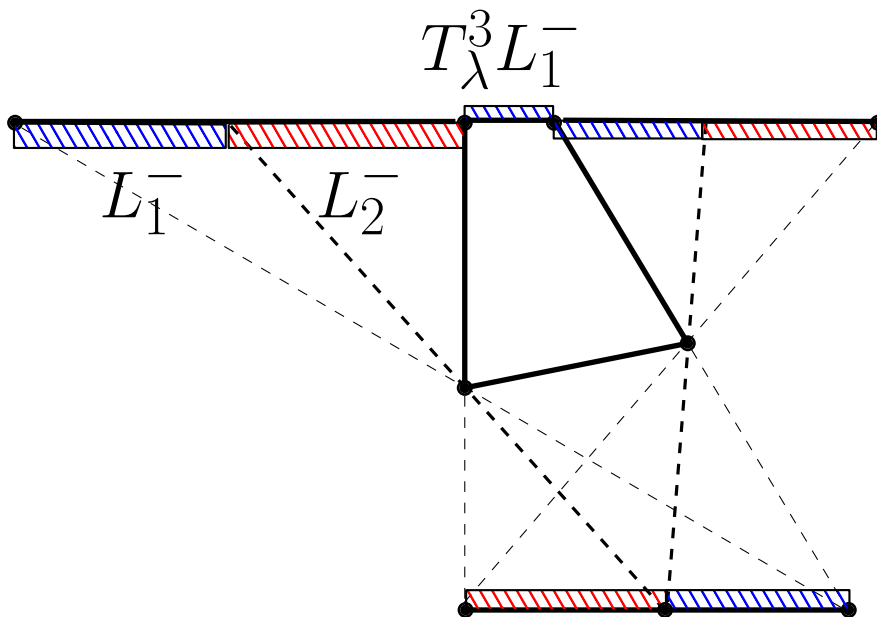


FIGURE 5.2. Dynamics of L_1^- and L_2^-

There is a natural partition $L^- = L_1^- \cup L_2^-$ (Figure 5.2), where L_1^- is defined to be the set of points that returns to L^- by T_λ^4 . For points in L_2^- , it takes T_λ^6 . The segment $T_\lambda^4 L_1^-$ (which is the T_λ -image of small segment

lying on top of \overline{AB} in Figure 5.2) might or might not intersect L_1^- , and the analysis gets simpler when it does not. This happens precisely when

$$(5.2) \quad a < \frac{\mu^2 + \mu^3}{1 + \mu^3 + \mu^4}$$

holds. In this section, we will only look at the space of quadrilaterals in X satisfying above inequality, which we denote by X_1 . Clearly, in the interval corresponding to L_1^- , g contracts by λ^4 and in the other interval, it contracts by λ^6 . Now notice that for any $(a, b) \in X$, $T_\lambda^3 L^+ \subset L^-$. So we can likewise consider the partition of L^+ into L_1^+ and L_2^+ , where $L_i^+ = (T_\lambda^3)^{-1}(L_i^-)$ for $i = 1, 2$. Let us point out that L_2^+ is located on the left of L_1^+ since T_λ^3 is orientation reversing. For $i = 1, 2$, we set f_i and g_i be the restriction of f and g onto L_i^+ and L_i^- , respectively.

Lemma 35. *For quadrilaterals in X_1 , we have relations*

$$\begin{aligned} T_\lambda^3 \circ f_2 &= g_2 \circ T_\lambda^3 \\ T_\lambda^3 \circ f_1 &= g_2 \circ g_1 \circ T_\lambda^3 \end{aligned}$$

where maps above are $L_2^+ \rightarrow L^-$ and maps below are $L_1^+ \rightarrow L^-$.

Proof. On L_2^+ , $f = T_\lambda^6$ since $T_\lambda^3 L_2^+ \subset L_2^-$ and $T_\lambda^3 L_2^- \subset L^+$. Similarly, on L_2^- , $g = T_\lambda^6$ so that $T_\lambda^3 \circ f_2 = g_2 \circ T_\lambda^3$ holds. For the second relation, we only need to take account of the fact that $T_\lambda^4(L_1^-) \subset L_2^-$. \square

Lemma 36. *For $(a, b) \in X_1$, there exist bijections between degenerate T_λ -periodic orbits intersecting $L(\epsilon)$, periodic orbits of f , and periodic orbits of g .*

Proof. Let \mathcal{O} be a T_λ -periodic orbit intersecting $L(\epsilon)$. By Lemma 30, $\mathcal{O} \cap L(\epsilon) = \mathcal{O} \cap L$. For each $p \in \mathcal{O} \cap L$, we can tell whether it corresponds to a point in L^+ or L^- by looking at its first three combinatorics. If it is $\{D, C, B\}$, $p \in L^-$ and otherwise $p \in L^+$ ($\{D, C, A\}$). Assume $p \in L^+$ for some $p \in \mathcal{O} \cap L$. Then the iterates $\{p, f(p), \dots\} \subset \mathcal{O} \cap L$ and it defines a single f -periodic orbit. It cannot exhaust the set $\mathcal{O} \cap L$ since $T_\lambda^3(p) \in L^-$. The remaining elements in $\mathcal{O} \cap L$ defines a single g -periodic orbit. We can deduce the same thing when we start by assuming $p \in L^-$.

Now, let \mathcal{U} be a periodic orbit for f . Pick any point $p \in \mathcal{U}$, then \mathcal{U} can be written as a finite letter $a_0 a_1 \dots a_{k-1}$ where k is the period and $a_l = i$ if and only if $f^l(p) \in L_i^+$ for $0 \leq l \leq k-1$. Then using relations from Lemma 35, it is straightforward to see that $q = T_\lambda^3 p$ is a periodic point of g with letter $b_0 \dots b_{l-1}$ obtained by applying the substitution

$$1 \mapsto 12 \quad 2 \mapsto 2$$

to the letter $a_0 \dots a_{k-1}$. That is, the periodic orbit \mathcal{U} for f has selected a periodic orbit \mathcal{V} of g , which is independent on the choice of p (a different choice would correspond to a cyclical permutation of letters). Then the union $\mathcal{U} \cup \mathcal{V}$ together with finitely many T_λ -iterates of it define a T_λ -periodic orbit intersecting $L(\epsilon)$. At this step, we note that any choice that g makes at the ambiguous point $1 - H/L$ is realized as a (degenerate) dynamics of T_λ . The same holds for f as well.

Finally, let \mathcal{V} be a g -periodic orbit. Pick a point $q \in \mathcal{V}$ and consider its letter as above. We have $g(L_1^-) \subset g(L_2^-)$ so that a 2 must follow whenever there is a 1 in this letter. That is, in any case we have $g^l(q) \in L_2^-$ for some l and then $p := T_\lambda^3(g^l(q)) \in L^+$. Then we see that p defines a f -periodic orbit, whose letter is the one obtained by applying the inverse substitution to the letter of q . \square

We claim that Lemma 36 also holds for quadrilaterals not in X_1 . To see this, first assume that the inequality 5.2 is not satisfied. Put $I = T_\lambda^4 L_1^- \cap L_1^-$ and $I' = (T_\lambda^4)^{-1}(I)$ so that I' is mapped homeomorphically onto I by $T_\lambda^4|_{I'}$, which is a translation composed with the contraction by λ^4 . Since I is always located to the right of I' and the right endpoint of I is the left endpoint of L_2^- , the homothety center of $T_\lambda^4|_{I'}$ is contained in the interior of L_2^- . In other words, for any $(a, b) \in X$, there exists an integer $N > 0$ such that L_1^- is partitioned into N intervals (from left to right) $L_{1,N}^-, \dots, L_{1,1}^-$ with the property that $(T_\lambda^4)^j L_{1,i}^- \subseteq L_1^-$ for $j < i$ and $(T_\lambda^4)^i L_{1,i}^- \subseteq L_2^-$.

We can denote X_N the subset of X that L_1^- is partitioned into N intervals as above, for $N \geq 1$. What depends on N is not the shape of the return map g (given by the equation 5.1) but the conjugacy relations between f and g . The explicit formulas are given by $N + 1$ relations for quadrilaterals in X_N ;

$$(5.3) \quad \begin{cases} T_\lambda^3 \circ f_2 & = g_2 \circ T_\lambda^3 \\ T_\lambda^3 \circ f_{11} & = g_2 \circ g_{11} \circ T_\lambda^3 \\ & \dots \\ T_\lambda^3 \circ f_{1N} & = g_2 \circ g_{1N} \circ \dots \circ g_{11} \circ T_\lambda^3 \end{cases}$$

where f_{1j} is the first-return map to $L_{1j}^+ = (T_\lambda^3)^{-1}L_{1j}^-$ for $1 \leq j \leq N$. These formulas are easily verified as in the simplest case $N = 1$. We note that Lemma 36 carries over to quadrilaterals in regions X_N ($N \geq 2$), using conjugacy relations. Therefore, using a result by Nogueira and Pires [9], we obtain the following corollary.

Corollary 37. *For $(a, b) \in X$, the number of T_λ -periodic orbits intersecting $L(\epsilon)$ cannot exceed 2.*

While it is easy to prove the finiteness of periodic orbits “away” from the singular rays (where the dynamics is continuous), the same question is highly nontrivial near the singular rays. Hence this result from [9] provides a case where the finiteness near a singular ray can be settled.

Now, we can also deduce the following corollary for all quadrilaterals in X .

Corollary 38. *Let $(a, b) \in X$. Every point in $L(\epsilon)$ is asymptotic to a degenerate T_λ -periodic orbit (resp. a Cantor set) if and only if the rotation number $\rho(g_{a,b})$ is rational (resp. irrational).*

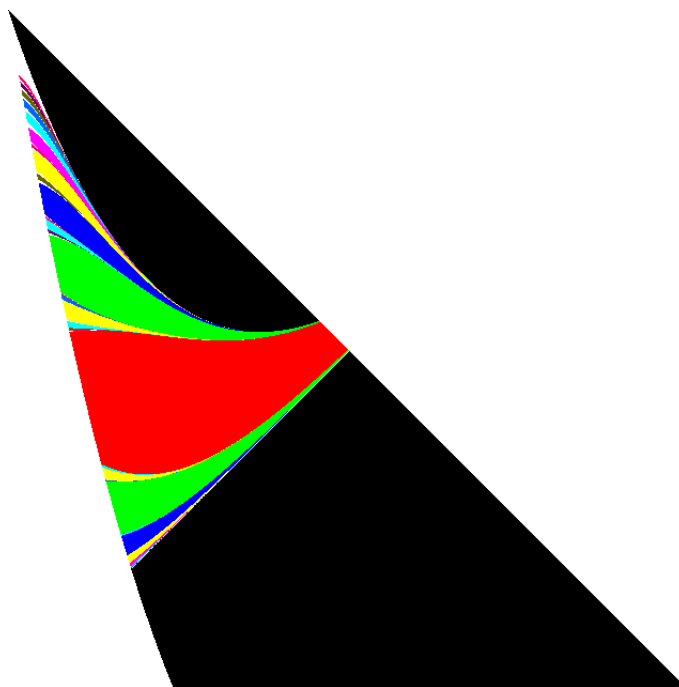


FIGURE 5.3. The rotation number as a function of parameters a and b . Here the vertical axis is a , the horizontal axis is b and the top left corner corresponds to $a = b = 0$.

Figure 5.3 shows the regions where the rotation number of $G_{a,b}$ is a rational number using various colors. In two black regions, the rotation numbers are 1 (upper region) and 0 (lower region). The central red region corresponds to $1/2$ and two green regions correspond to $2/3$ and $1/3$, and so on. It follows from continuity that for each irrational number $0 < \alpha < 1$, there exists a 1-parameter family of quadrilaterals whose first-return maps have rotation number α . We note that if the rotation number of g is rational and has denominator d , then the corresponding degenerate T_λ -periodic orbit has period greater than $3d$.

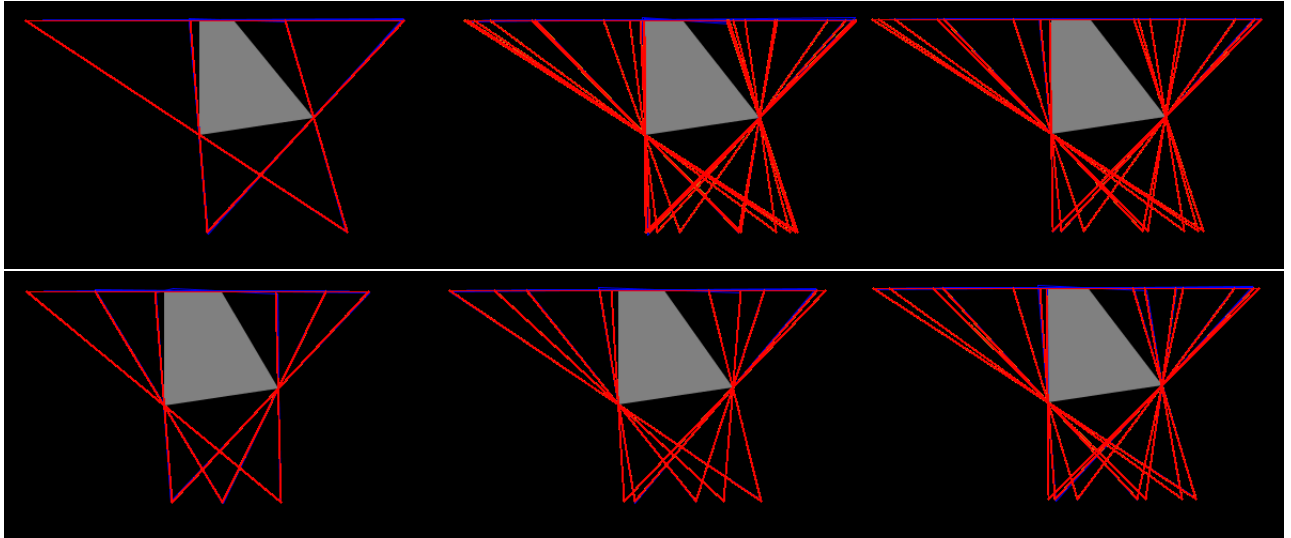


FIGURE 5.4. The bifurcation attracting periodic orbits are drawn for $P = (a, b = 0.15)$ where $a = 0.30, 0.33, 0.34, 0.35, 0.40, 0.50$ in clockwise order starting from the top left picture. They correspond to rotation numbers $1, 6/7, 4/5, 3/4, 2/3, 1/2$, respectively. One can easily see that the period increases in proportion to the denominator of the rotation number.

ACKNOWLEDGMENTS

Around 75% of this work was done when I was participating at Summer @ ICERM program in its initiation year 2012. ICERM really provides the ideal mathematics research environment.

Two faculty advisors of this program were Prof. Sergei Tabachnikov and Prof. Pat Hooper and this project was simply impossible without their guidance. Prof. Tabachnikov is a true expert on the outer billiards problem and he was the one who has proposed this problem of outer billiards with contraction and formulated a few conjectures. Prof. Hooper is a brilliant and inventive dynamicist and he has worked on the inner billiards problem, which is dual to the outer billiards problem in several ways. His various insights and observations were extremely helpful in my research. In particular, he was the one who first anticipated the existence of attracting Cantor sets. His guidance was essential for the eventual proof of existence of such Cantor sets. It should be emphasized that the computer program developed by Prof. Hooper played a crucial role. As a matter of fact, most of the results presented here depended on the experiments based on the program.

It is such a coincidence that Prof. Richard Schwartz, who had previously made breakthroughs both in inner and outer billiards problem, was a professor at Brown. He visited the institute very often, and we had numerous discussions which helped me significantly. Especially he pointed out to me the existence of exotic periodic tiles outside the regular septagon. He has also modified his computer program on outer billiards for me and this was a very useful tool to have. He is also my thesis advisor and read the drafts several times at various stages. His comments has significantly improved the quality of this thesis. But more importantly, his dedication and passion for mathematics has motivated me throughout this project.

Graduate student advisors Tarik Aougab and Diana Davis were very friendly and helpful. They have commented on my drafts several times and also advised me on presentation skills.

I had two other students in my research group, Francisc Bozgan and Julienne Lachance. They were interested in different aspects of the outer billiards with contraction system which was helpful. Fransics gave me a lot of motivation throughout the program and we also proved a couple of facts together. Julienne expanded the computer program of Prof. Hooper which has turned out to be very useful.

I also thank Prof. Nicolas Bedaride and Yilong Yang for discussions and interest in my project.

Finally I want to thank Prof. Schwartz and Prof. Hooper once again for making me realize the power of computer experimentation in mathematics.

Let me acknowledge that Figures 1.1, 4.2, 4.5, and 4.10 were produced either by Prof. Schwartz or by his computer program. Figures 3.3, 3.5, 4.6, 4.11, 4.13, 4.15, 4.16, 4.17, and 5.4 were produced by the program by Prof. Hooper and Julienne. Also the beautiful coloring scheme of Figure 5.3 was provided by Prof. Hooper.

APPENDIX A. PROOF OF THEOREM 25.

Proof. We will first prove that for $\lambda > 1/(1 + 2\cos(2\pi/n))$, there exist two star shaped orbits. Next, we need to show that for $\lambda \leq 1/(1 + 2\cos(2\pi/n))$, the Fagnano orbit attracts the whole domain. This statement is harder to prove, and our proof consists of a geometric part and an analytic part.¹

The value $\lambda = 1/(1 + 2\cos(2\pi/n))$ is chosen to satisfy $|B'D| \times \lambda = |DD'|$ in Figure 5.5. Given a regular $n \geq 5$ gon P , we connect its shortest diagonal to obtain a smaller regular n -gon P' inside as shown in figure 4.12. Given any $0 < \lambda < 1$, we can construct yet another regular n -gon P'' by dividing each edge of P' with ratio $1 : \lambda$. Then P is a $T_{\lambda'}$ -periodic orbit around P'' for λ' determined by λ , and we see that when λ goes to 1, λ' approaches $1/(1 + 2\cos(2\pi/n))$.

Now let us prove the second statement. Notice that for all values of n , small triangles formed by taking the intersection of extensions of two edges adjacent to one edge ($\triangle AA'B$, $\triangle BB'C$, ... in Figure 5.5) are basin of attraction for $\lambda > 1/(1 + 2\cos(2\pi/n))$. The following proof requires that $n \geq 8$. For $n = 5, 6$, and 7 , a finite computation shows that the ball of radius 2 centered at the origin is covered by taking second inverse iterates of aforementioned triangle regions.

When $n \geq 8$, the rays BB' and DC' intersect, and let us call it B'' . The point C'' is constructed similarly. Now we claim that the inverse image of $\triangle EDD'$ contains $\triangle DB'B''$. Our λ is chosen in a way that $|B'D| \times \lambda = |DD'|$, and when $n \geq 8$, the angle between rays ED' and BB' are $8\pi/n$ which does not exceed π . Therefore, the inverse image of $\triangle EDD'$ is a triangle containing $\triangle DB'B''$. We now consider $\triangle BFG$, which is obtained as the inverse image of $\triangle BB''C'$, which is now known to be a basin of attraction. Consider the line OH perpendicular to edge ED . Since ED is parallel to FG , the line OH will intersect with the extension of FG at a point which lies on the opposite side of G with respect to F . Hence F is the point whose distance to O is minimal. Consider all $2\pi k/n$ -rotated images of $\triangle FGB$ with respect to O , whose union is now a basin of attraction. It is elementary to see that the segment FO is contained in this union. (if we counterclockwise rotate the segment FB by $2\pi/n$, this rotated segment will intersect the segment FO in its interior, and so on) Therefore, it implies that this union contains the ball of radius $|FO|$ centered at O . Let us call this radius by d_1 .

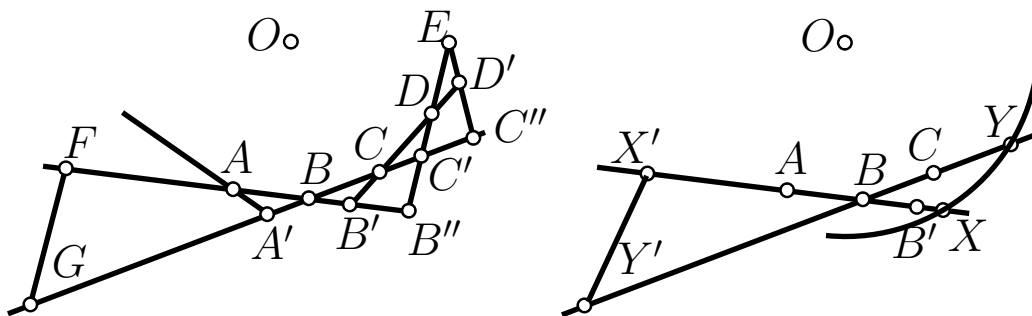


FIGURE 5.5. Geometric part of the proof

Now consider a situation where some ball radius $d > 1$ centered at O is given as a basin of attraction. The circle of radius d will intersect rays BB' and BC at two points X and Y respectively (Figure 5.5, right). Since the triangle BXY is contained in this ball, the inverse image $\triangle BX'Y'$ is also a basin of attraction. By the same logic, we consider all its $2\pi/n$ -rotates and argue that on the segment $X'Y'$, X' is the closest to O and that the segment $X'O$ is contained in the union of rotated images. That is, we now know that the whole ball of radius $h(d) = |OX'|$ centered at O is a basin of attraction. Here h is simply a function converting a number greater than 1 to another number.

¹Regarding this analytic part: I had to show that some function was always positive, so I consulted R. Schwartz to set up a computer-aided proof. On the other hand, F. Bozgan thought it is possible by hand, and he managed to do it in a few hours.

Since we have our initial radius $d_1 > 1$ to begin with, we apply above procedure to get a sequence of radii $h(d_1), h(h(d_1)), \dots$, which we want to prove that it goes to infinity. It will be enough to prove that for $d \geq d_1$, the function $f(d) := h(d)/d$ is strictly greater than 1 and non decreasing for all $n \geq 8$. From now on, the proof is technical. We will show that $f(d_1) > 1$ for all $n \geq 8$ and f is increasing for $d \geq d_1$. Three following lemmas will complete the proof. \square

Lemma 39. *For each n , we have the following formula for d_1 :*

$$\sqrt{\cos^2\left(\frac{\pi}{n}\right) + \sin^2\left(\frac{\pi}{n}\right)\left\{\left(\frac{1 + 2\cos(2\pi/n)}{\cos(2\pi/n)}\right)\left(1 + \frac{\cos(\pi/n)}{\cos(3\pi/n)}\right) - 1\right\}^2}.$$

Proof. Straightforward verification. \square

Lemma 40. *For each n , we have*

$$f^2(d) = \frac{1}{d^2}\left(1 + \frac{1}{\lambda}\right)\left(1 + \frac{(\sqrt{d^2 - \cos^2(\pi/n)} - \sin(\pi/n))^2}{\lambda}\right) - \frac{1}{\lambda}.$$

Proof. We look at triangles $\triangle OX'B$ and $\triangle OXB$. From the law of cosines, we have

$$h(d)^2 = 1^2 + x^2/\lambda^2 - 2(x/\lambda)\cos(\angle OBX')$$

and

$$d^2 = 1^2 + x^2 + 2x\cos(\angle OBX),$$

where we temporarily denote $|BX| = x$. Multiply the first equation by λ and add two equations to obtain $\lambda h(d)^2 + d^2 = (1 + \lambda) + x^2(1 + 1/\lambda)$. The length of BX is obtained by taking the square root of $|OX|^2 - |OM|^2$ and subtracting $\sin(\pi/n)$, where M is the midpoint of AB . \square

Lemma 41. *For each n , $f(d_1) > 1$ and $f(d)$ is increasing for $d \geq d_1$.*

Proof. Since it is clear that $f > 0$, it is enough to show that $f(d_1)^2 > 1$ and $f(d)^2$ is increasing, or $(f(d)^2)' > 0$ for $d \geq d_1$. We begin by showing that $f(d_1)^2 > 1$. It is equivalent to showing that

$$\begin{aligned} & \frac{1}{d^2}\left(\frac{1}{\lambda} + 1\right)\left(1 + \frac{(\sqrt{d^2 - \cos^2(\pi/n)} - \sin(\pi/n))^2}{\lambda}\right) > 1 + \frac{1}{\lambda} \\ \iff & 1 + \frac{(\sqrt{d^2 - \cos^2(\pi/n)} - \sin(\pi/n))^2}{\lambda} > d^2 \\ \iff & 1 + (1 + 2\cos(\frac{2\pi}{n}))(d^2 - \cos(\frac{2\pi}{n}) - 2\sin(\frac{\pi}{n})\sqrt{d^2 - \cos^2(\frac{\pi}{n})}) > d^2 \\ \iff & 1 - 2\cos^2(\frac{2\pi}{n}) - \cos(\frac{2\pi}{n}) + 2d^2\cos(\frac{2\pi}{n}) \\ & - 2\sin(\frac{\pi}{n})(1 + 2\cos(\frac{2\pi}{n}))\sqrt{d^2 - \cos^2(\frac{\pi}{n})} > 0 \\ \iff & 2\cos(\frac{2\pi}{n})d^2 - 2\sin(\frac{\pi}{n})(1 + 2\cos(\frac{2\pi}{n}))\sqrt{d^2 - \cos^2(\frac{\pi}{n})} > \cos(\frac{2\pi}{n}) + \cos(\frac{4\pi}{n}) \\ \iff & 2\cos(\frac{2\pi}{n})\cos^2(\frac{\pi}{n}) + 2\cos(\frac{2\pi}{n})\left\{\left((G(n) + 1)\sin(\frac{\pi}{n}) - \sin(\frac{\pi}{n})\right)^2\right. \\ & \left. - 2\sin(\frac{\pi}{n})(1 + 2\cos(\frac{2\pi}{n}))G(n)\right\} > \cos(\frac{2\pi}{n}) + \cos(\frac{4\pi}{n}), \end{aligned}$$

where we are introducing

$$G(n) = \left(\frac{1 + 2\cos(2\pi/n)}{\cos(2\pi/n)}\right)\left(1 + \frac{\cos(\pi/n)}{\cos(3\pi/n)}\right) - 1.$$

Continuing with our original expression, we get

$$\iff \sin^2\left(\frac{2\pi}{n}\right) + 2\cos\left(\frac{2\pi}{n}\right)\sin^2\left(\frac{\pi}{n}\right)G(n)^2 - 2\sin^2\left(\frac{\pi}{n}\right)(1 + 2\cos\left(\frac{2\pi}{n}\right))G(n) > 0.$$

Write $\sin^2\left(\frac{2\pi}{n}\right) = (2\sin\left(\frac{\pi}{n}\right)\cos\left(\frac{\pi}{n}\right))^2$ to cancel $\sin^2\left(\frac{2\pi}{n}\right)$. Use the substitution $2\cos^2\left(\frac{\pi}{n}\right) = \cos\left(\frac{2\pi}{n}\right) + 1$ and then we are left with

$$\begin{aligned} \iff & 2\cos\left(\frac{2\pi}{n}\right) + 2 + 2\cos\left(\frac{2\pi}{n}\right)G(n)^2 - 2(1 + 2\cos\left(\frac{2\pi}{n}\right))G(n) > 0 \\ \iff & (2\cos\left(\frac{2\pi}{n}\right) + 1) + (2\cos\left(\frac{2\pi}{n}\right) + 1)G(n)^2 + 2(1 + 2\cos\left(\frac{2\pi}{n}\right))G(n) > G(n)^2 - 1 \\ \iff & (2\cos\left(\frac{2\pi}{n}\right) + 1)(G(n) - 1)^2 > G(n)^2 - 1 \\ \iff & (2\cos\left(\frac{2\pi}{n}\right) + 1)(G(n) - 1) > G(n) + 1. \\ \iff & \left(\frac{1 + 2\cos(2\pi/n)}{\cos(2\pi/n)}\right)\left(1 + \frac{\cos(\pi/n)}{\cos(3\pi/n)}\right) - 1 = G(n) > \frac{1 + \cos(2\pi/n)}{\cos(2\pi/n)} \\ \iff & \left(\frac{1 + 2\cos(2\pi/n)}{\cos(2\pi/n)}\right)\left(1 + \frac{\cos(\pi/n)}{\cos(3\pi/n)}\right) > \frac{1 + 2\cos(2\pi/n)}{\cos(2\pi/n)} \\ \iff & 1 + \frac{\cos(\pi/n)}{\cos(3\pi/n)} > 1. \end{aligned}$$

Since $G(n) - 1 > 4$, we could divide by it. Hence we are done with this part. It is straightforward to verify that the derivative of $f(d)^2$ is, when we factor out a positive part, equals

$$h(d) := \cos\left(\frac{2\pi}{n}\right) - \frac{1}{1 + 2\cos(2\pi/n)} + \sin\left(\frac{\pi}{n}\right)\left(\frac{d^2 - 2\cos^2(\pi/n)}{\sqrt{d^2 - \cos^2(\pi/n)}}\right)$$

which we want to show positive for $d \geq d_1$. For this it is enough to show that $h(d_1) > 0$ and $h'(d) > 0$ for $d > 0$. For the latter part, we have

$$h'(d) = \frac{d^3}{(x^2 - \cos^2(2\pi/n))^{3/2}} > 0,$$

so we only need to check $h(d_1) > 0$. This statement is equivalent to:

$$\begin{aligned} & \frac{\cos(2\pi/n) + 2\cos^2(2\pi/n) - 1}{1 + 2\cos(2\pi/n)} + \sin\left(\frac{\pi}{n}\right)\left(\frac{d^2 - 2\cos^2(\pi/n)}{\sqrt{d^2 - \cos^2(\pi/n)}}\right) > 0 \\ \iff & \frac{\cos(2\pi/n) + \cos(4\pi/n)}{1 + 2\cos(2\pi/n)} + \sin\left(\frac{\pi}{n}\right)\frac{(y - \sin(\pi/n))^2 - \cos^2(\pi/n)}{(y - \sin(\pi/n))} > 0, \end{aligned}$$

where y is simply given by the relation $d^2 = \cos^2(\pi/n) + (y - \sin(\pi/n))^2$:

$$\begin{aligned} \iff & \frac{2\cos(\pi/n)\cos(3\pi/n)}{1 + 2\cos(2\pi/n)} + \sin\left(\frac{\pi}{n}\right)(y - \sin\left(\frac{\pi}{n}\right)) - \frac{\cos^2(\pi/n)}{G(n)} > 0 \\ \iff & \frac{2\cos(\pi/n)\cos(3\pi/n)}{1 + 2\cos(2\pi/n)} + \sin^2\left(\frac{\pi}{n}\right)G(n) - \frac{\cos^2(\pi/n)}{\left(\frac{1 + 2\cos(2\pi/n)}{\cos(2\pi/n)}\right)\left(1 + \frac{\cos(\pi/n)}{\cos(3\pi/n)}\right) - 1} > 0 \end{aligned}$$

Let us simplify the last term:

$$\begin{aligned}
& \frac{\cos^2(\pi/n) \cos(3\pi/n)}{(1 + 2 \cos(2\pi/n))2 \cos(\pi/n) - \cos(3\pi/n)} \\
&= \frac{\cos(\pi/n) \cos(3\pi/n)}{2(1 + 2 \cos(2\pi/n)) - 4 + 3 \cos^2(\pi/n)} \\
&= \frac{2 \cos(\pi/n) \cos(3\pi/n)}{11 \cos(2\pi/n) - 1}.
\end{aligned}$$

Therefore, our expression equals

$$\begin{aligned}
& \iff \frac{2 \cos(\pi/n) \cos(3\pi/n)}{1 + 2 \cos(2\pi/n)} + \sin^2\left(\frac{\pi}{n}\right)G(n) - \frac{2 \cos(\pi/n) \cos(3\pi/n)}{11 \cos(2\pi/n) - 1} > 0 \\
& \iff \sin^2\left(\frac{\pi}{n}\right)G(n) + \frac{2 \cos(\pi/n) \cos(3\pi/n)}{(1 + 2 \cos(2\pi/n))(11 \cos(2\pi/n) - 1)}(9 \cos(2\pi/n) - 2) > 0.
\end{aligned}$$

This final expression is easily seen to be positive: the first term is clearly positive, and $n \geq 8$ so $9 \cos(2\pi/n) - 2 > 0$. Indeed, $h(d_1)$ monotonically decreases to the limit $7/15$. \square

APPENDIX B. ROTATION THEORY FOR DISCONTINUOUS CIRCLE MAPS

Recall that the rotation number for a circle homeomorphism $f : S^1 \rightarrow S^1$ is defined by

$$(5.4) \quad \rho(F) = \lim_{n \rightarrow \infty} \frac{F^n(x) - x}{n}$$

where F is any lift of f into a homeomorphism of \mathbb{R} and x is an arbitrary real number. Once we fix F , this limit exists and independent on x . If we have two lifts F_1 and F_2 , $\rho(F_1) - \rho(F_2)$ is an integer so that the rotation number of f , $\rho(f)$ is uniquely determined mod 1. Then, $\rho(f)$ is rational if and only if f has a periodic point. On the other hand, when $\rho(f)$ is irrational, the ω -limit set of a point (which is independent on the point) is either the whole circle or a Cantor set.

Rhodes and Thompson, in [10, 11], develops a theory of rotation number for a large class of functions $f : S^1 \rightarrow S^1$. We only state the results that we need. A map (not necessarily continuous) $f : S^1 \rightarrow S^1$ is in class \mathcal{S} if and only if it has a lift $F : \mathbb{R} \rightarrow \mathbb{R}$ such that F is strictly increasing and $F(x+1) = F(x) + 1$ for all $x \in \mathbb{R}$. Now given such a lift F , since it is strictly increasing, we can define F^- and F^+ , where they are continuous everywhere from the left and from the right, respectively and coincide with F whenever F is continuous. Then we consider the filled-graph of F defined by

$$\Gamma(F) := \{(x, y) | 0 \leq x \leq 1, F^-(x) \leq y \leq F^+(x)\}$$

which is simply the graph of F where all the jumps are filled with vertical line segments. We have restricted the set to the region $0 \leq x \leq 1$ to make it compact. We will consider the Hausdorff metric on the collection of $\Gamma(F)$ where F is some lift of $f \in \mathcal{S}$.

Theorem. [10] *The rotation number $\rho(f)$ is well-defined for $f \in \mathcal{S}$ up to mod 1 by the equation 5.4 where F is any strictly increasing degree 1 lift of f . This number does not change if we redefine f at its points of discontinuity.*

Moreover, $\rho(f)$ is rational if and only if there exists some function \tilde{f} which has a periodic point, where \tilde{f} coincides with f possibly except at finitely many points where f is discontinuous.

Theorem. [11] *Let F_λ be a family of strictly increasing degree 1 functions $\mathbb{R} \rightarrow \mathbb{R}$ for $\lambda = [0, 1]$. If $\Gamma(F_\lambda) \rightarrow \Gamma(F_0)$ as $\lambda \rightarrow 0$ in the Hausdorff topology, then $\rho(F_\lambda) \rightarrow \rho(F_0)$.*

Notice that when the family F_λ is uniformly convergent, $\Gamma(F_\lambda)$ clearly converges to $\Gamma(F_0)$ in the Hausdorff topology. Finally, regarding the ω -limit set we refer to [1].

Theorem. [1] *If $f \in \mathcal{S}$ has a rational rotation number p/q , $\omega(x)$ gives a q -periodic orbit of \tilde{f} (which exists by above result) for all $x \in S^1$. If f has an irrational rotation number, $\omega(x) = \omega(y)$ for all $x, y \in S^1$ and it is either S^1 or a Cantor set.*

REFERENCES

- [1] Romain Brette. Rotation numbers of discontinuous orientation-preserving circle maps. *Set-Valued Analysis*, Volume 11, Number 4:359–371, 2003.
 - [2] Henk Bruin and Jonathan H. B. Deane. Piecewise contractions are asymptotically periodic. *Proc. Amer. Math. Soc.*, 137(4):1389–1395, 2009.
 - [3] Christopher Chase, Joseph Serrano, and Peter J. Ramadge. Periodicity and chaos from switched flow systems: contrasting examples of discretely controlled continuous systems. *IEEE Trans. Automat. Control*, 38(1):70–83, 1993.
 - [4] Daniel Genin. Research announcement: boundedness of orbits for trapezoidal outer billiards. *Electron. Res. Announc. Math. Sci.*, 15:71–78, 2008.
 - [5] Daniel I. Genin. *Regular and chaotic dynamics of outer billiards*. ProQuest LLC, Ann Arbor, MI, 2005. Thesis (Ph.D.)—The Pennsylvania State University.
 - [6] Eugene Gutkin and Nándor Simányi. Dual polygonal billiards and necklace dynamics. *Comm. Math. Phys.*, 143(3):431–449, 1992.
 - [7] Jürgen Moser. Is the solar system stable? *Math. Intelligencer*, 1(2):65–71, 1978/79.
 - [8] Julien Cassaigne Nicolas Bedaride. Outer billiard outside regular polygons. *J. London Math. Soc.*, 2011.
 - [9] Arnaldo Nogueira and Benito Pires. Dynamics of piecewise contractions of the interval, 2012.
 - [10] Frank Rhodes and Christopher L. Thompson. Rotation numbers for monotone functions on the circle. *J. London Math. Soc. (2)*, 34(2):360–368, 1986.
 - [11] Frank Rhodes and Christopher L. Thompson. Topologies and rotation numbers for families of monotone functions on the circle. *J. London Math. Soc. (2)*, 43(1):156–170, 1991.
 - [12] Richard Evan Schwartz. Obtuse triangular billiards. I. Near the (2, 3, 6) triangle. *Experiment. Math.*, 15(2):161–182, 2006.
 - [13] Richard Evan Schwartz. *Outer billiards on kites*, volume 171 of *Annals of Mathematics Studies*. Princeton University Press, Princeton, NJ, 2009.
 - [14] Richard Evan Schwartz. Outer billiards, arithmetic graphs, and the octagon, 2010.
 - [15] Richard Evan Schwartz. Outer billiards and the pinwheel map. *J. Mod. Dyn.*, 5(2):255–283, 2011.
 - [16] S. Tabachnikov. On the dual billiard problem. *Adv. Math.*, 115(2):221–249, 1995.
 - [17] Serge Tabachnikov. Billiards. *Panor. Synth.*, (1):vi+142, 1995.
 - [18] Serge Tabachnikov. Fagnano orbits of polygonal dual billiards. *Geom. Dedicata*, 77(3):279–286, 1999.
 - [19] Serge Tabachnikov. *Geometry and billiards*, volume 30 of *Student Mathematical Library*. American Mathematical Society, Providence, RI, 2005.
 - [20] Serge Tabachnikov. A proof of Culter’s theorem on the existence of periodic orbits in polygonal outer billiards. *Geom. Dedicata*, 129:83–87, 2007.
 - [21] Peter Veerman. Symbolic dynamics of order-preserving orbits. *Phys. D*, 29(1-2):191–201, 1987.
- E-mail address:* in-jee_jeong@brown.edu